Journal Pre-proof

Tracing natural and anthropogenic sources of aerosols to the Atlantic Ocean using Zn and Cu isotopes

Hollie Packman, Susan H. Little, Alex R. Baker, Luke Bridgestock, Rosie J. Chance, Barry J. Coles, Katharina Kreissig, Mark Rehkämper, Tina van de Flierdt
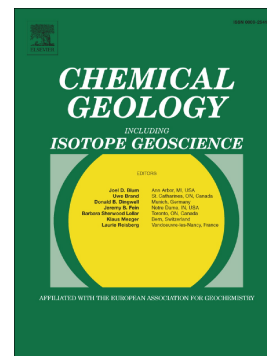
Please cite this article as: H. Packman, S.H. Little, A.R. Baker, et al., Tracing natural and anthropogenic sources of aerosols to the Atlantic Ocean using Zn and Cu isotopes, *Chemical Geology* (2022), https://doi.org/10.1016/j.chemgeo.2022.121091

This is a PDF file of an article that has undergone enhancements after acceptance, such as the addition of a cover page and metadata, and formatting for readability, but it is not yet the definitive version of record. This version will undergo additional copyediting, typesetting and review before it is published in its final form, but we are providing this version to give early visibility of the article. Please note that, during the production process, errors may be discovered which could affect the content, and all legal disclaimers that apply to the journal pertain.

Tracing natural and anthropogenic sources of aerosols to the Atlantic Ocean using Zn and Cu isotopes

Hollie Packman[a,b], Susan H. Little[b,c,*], Alex R. Baker[d], Luke Bridgestock[e], Rosie J. Chance[d,f], Barry J. Coles[b], Katharina Kreissig[b], Mark Rehkämper[b], Tina van de Flierdt[b]

[a]Science and Solutions for a Changing Planet Doctoral Training Partnership, Grantham Institute - Climate Change and the Environment, Imperial College London, Exhibition Road, South Kensington, London SW7 2AZ

[b]Department of Earth Science and Engineering, Imperial College London, South Kensington Campus, London, SW7 2AZ, UK

[c]Department of Earth Sciences, University College London, Gower Street, London, WC1E 6BT, UK

[d]Centre for Ocean and Atmospheric Sciences, School of Environmental Sciences, University of East Anglia, Norwich Research Park, Norwich, NR4 7TJ, UK

[e]Department of Earth Sciences, University of Cambridge, Downing Street, Cambridge, CB2 3EQ, UK

[f]Wolfson Atmospheric Chemistry Laboratories, Department of Chemistry, University of York, York, YO10 5DD, UK

*Corresponding author (susan.little@ucl.ac.uk)

Abstract

Anthropogenic activities have significantly enhanced atmospheric metal inputs to the ocean, which has potentially important consequences for marine ecosystems. This study assesses the potential of Zn and Cu isotope compositions to distinguish between natural and anthropogenic atmospheric inputs of these metals to the surface ocean. To this end, the isotopic compositions of Zn and Cu in aerosols collected from the eastern tropical Atlantic Ocean on the GEOTRACES GA06 cruise are examined. Enrichment factors and fractional solubility measurements indicate the presence of a significant anthropogenic component in the aerosols collected furthest from the North African dust plume for both Zn and Cu. The mean $\delta^{65}Cu_{\text{NIST SRM 976}}$ for the fully digested aerosols is +0.07 ± 0.39 ‰ (n = 9, 2 SD), which is indistinguishable from the lithogenic value, and implies that Cu isotopes are not an effective tracer of aerosol sources in this region. The mean $\delta^{66}Zn_{\text{JMC-Lyon}}$ value for the aerosols that underwent a total digestion is +0.17 ± 0.22 ‰ (n = 11, 2 SD). The aerosols leached with ammonium acetate have similar Zn isotope compositions, with a mean of +0.15 ± 0.16 ‰ (n = 7, 2 SD). The aerosols were collected in a region with prevalent mineral dust but, despite this, exhibit isotopically lighter Zn than lithogenic Zn with $\delta^{66}Zn \approx$ +0.3 ‰. When coupled with the previously published Pb isotope data, the aerosols exhibit coupled Zn-Pb isotope systematics that are indicative of mixing between mineral dust ($\delta^{66}Zn$ = +0.28 ‰ and $^{206}Pb/^{207}Pb$ = 1.205) and anthropogenic emissions ($\delta^{66}Zn$ = -0.22 ‰ and $^{206}Pb/^{207}Pb$ = 1.129). This demonstrates the potential of Zn isotopes to trace atmospheric Zn inputs from anthropogenic sources to the surface ocean.

Keywords: Aerosols; Zinc; Copper; isotopic composition; anthropogenic contribution; trace metals

1 Introduction

Zinc and Cu are essential micronutrients for marine algae (e.g., Moore et al., 2013). Zinc is present as a

cofactor in several key enzymes in phytoplankton, including carbonic anhydrase which catalyses the

interconversion of carbon dioxide, and alkaline phosphatase which catalyses the hydrolysis of phosphate

esters (Sunda, 1989; Vallee and Auld, 1990). Copper also has multiple biological functions, for example,

in electron transport chains for photosynthetic and respiratory processes (Lopez et al., 2019). However,

the free Cu^{2+} ion is toxic at low concentrations (Sunda, 1976; Brand et al., 1986; Paytan et al., 2009).

Phytoplankton combat the toxicity of Cu(II) by releasing strong organic ligands that complex >99% of

dissolved Cu in seawater (e.g., Coale and Bruland, 1988; Moffett and Brand, 1996; Moffett and Dupont,

2007).

There are two primary external supply routes of trace metal micronutrients to the surface ocean: via

rivers (e.g., Chester and Jickells, 2012) and via the atmospheric deposition of aerosols (e.g., Duce et al.,

1991; Jickells, 1995). Both these input fluxes have been significantly enhanced by anthropogenic

activities (e.g., Nriagyu and Pacyna, 1988; Pacyna and Pacyna, 2001). However, distinguishing and

quantifying natural and anthropogenic sources of Cu and Zn to the ocean is challenging (Little et al.,

2014; Mahowald et al., 2018). Stable isotope measurements of Zn and Cu have been vital in

comprehending their marine biogeochemical cycles and may therefore be useful in investigating their

atmospheric inputs.

Zinc has a typical 'nutrient-type' profile in seawater, with concentrations that are up to 1400 times

higher in the deep oceans than the surface, attributed to the impact of biological uptake and

regeneration superimposed on the physical ocean circulation (e.g., Bruland, Middag and Lohan, 2013;

Roshan et al., 2018; Weber et al., 2018). Away from sedimentary and hydrothermal Zn sources, deep

ocean Zn isotope compositions are generally homogeneous, at $\delta^{66}Zn$ = +0.45 ± 0.14 ‰ (e.g., John and

Conway, 2014; Zhao et al., 2014; Vance et al., 2019). Zinc isotope ratios typically show a minimum in the

sub-surface (e.g., John and Conway, 2014; Vance et al., 2019), with the exception of the Southern Ocean

(e.g., Wang et al., 2019; Sieber et al., 2020). These isotopically light sub-surface Zn isotope compositions

have been explained in terms of (a) scavenging of isotopically heavy Zn (e.g., John and Conway, 2014;

Weber et al., 2018; Liao et al., 2020), (b) the shallow remineralisation of isotopically light Zn (Samanta et

al., 2017; Vance et al., 2019), or (c) as the result of an external source of isotopically light Zn (Lemaitre et

al., 2020; Liao et al., 2020). Aerosols of anthropogenic origin are one possible source of isotopically light

Zn (e.g., John et al., 2007; Mattielli et al., 2009; Lemaitre et al., 2020).

The vertical dissolved Cu distribution in the ocean has been described as 'hybrid-type', due to the

combination of its role as a nutrient and its particle scavenging reactivity (Bruland et al., 2013).

Anthropogenic Cu sources increase oceanic Cu concentrations, with some models predicting reduced

phytoplankton growth rates in strongly Cu-contaminated regions (Moffett et al., 1997; Paytan et al.,

2009; Jordi et al., 2012). The varying sensitivity of different groups of phytoplankton to Cu toxicity can

influence the ecological composition in a region (Quigg et al., 2006; Levy et al., 2007; Wang et al., 2017).

The deep ocean is isotopically homogenous for Cu, with $\delta^{65}Cu$ values of about +0.6 to +0.7 ‰ (e.g.,

Thompson, Ellwood and Wille, 2013; Takano et al., 2014; Little et al., 2018; Baconnais et al., 2019).

Upper-ocean Cu isotope compositions generally show deviations towards lower $\delta^{65}Cu$ (about +0.3 to

+0.4 ‰), which have been interpreted as reflecting the input of isotopically light particulate Cu, either

via aerosols or rivers (e.g., Takano et al., 2014; Little et al., 2018).

The eastern tropical Atlantic receives atmospheric particles from diverse natural and anthropogenic

sources. One major natural source is mineral dust from the Sahara desert (Laurent et al., 2008). Globally,

mineral dust shows some geographical variations in Zn isotope compositions, but $\delta^{66}Zn$ values are

positive and fall near the lithogenic Zn isotope composition, of +0.28 ± 0.26 ‰ (n = 105, 2 SD; Moynier

et al., 2017). The few published Zn isotope compositions of Saharan dust exhibit $\delta^{66}Zn$ values of +0.43 ±

0.10 ‰ (n = 6, 2 SD; Dong et al., 2013) and +0.19 ± 0.29 ‰ (n = 4, 2 SD; Schleicher et al., 2020). Mineral

dust δ^{65}Cu values are also similar to the lithogenic value, of +0.08 ± 0.40 ‰ (n = 42, 2 SD; Moynier et al., 2017), with reported Saharan dust δ^{65}Cu values of -0.24 ± 0.11 ‰ (n = 6, 2 SD; Dong et al., 2013) and -0.01 ± 0.28 ‰ (n = 4, 2 SD; Schleicher et al., 2020).

A significant proportion of atmospheric particles originate from anthropogenic activities, e.g., fossil fuel burning, vehicular traffic, pyrometallurgical production (Nriagu and Pacyna, 1988; Pacyna and Pacyna, 2001). The predominant anthropogenic source of atmospheric Zn and Cu is non-ferrous metal production, for example in Zn-Pb refineries (Nriagu, 1979; Pacyna and Pacyna, 2001; Shiel et al., 2010). It is well established that the pyrometallurgical process fractionates Zn isotopes (John et al., 2007; Shiel et al., 2010). Studies have reported that the δ^{66}Zn values of anthropogenic contaminants are lower than the lithogenic background (Cloquet et al., 2006a; John et al., 2007; Chen et al., 2008; Mattielli et al., 2009; Bigalke et al., 2010; Borrok et al., 2010; Thapalia et al., 2010; Ochoa Gonzalez et al., 2016; Souto-Oliveira et al., 2018; Gelly et al., 2019; Souto-Oliveira et al., 2019). As Cu has a higher boiling point (2595 °C) than Zn (907 °C), it has been posited that combustion processes, such as in smelters (1000-1150 °C), do not fractionate the isotopes of Cu to the same extent as is observed for Zn (Mattielli et al., 2009; Thapalia et al., 2010; Gelly et al., 2019).

In this study, we report the Zn and Cu isotope compositions of aerosol samples from the eastern tropical Atlantic Ocean. The solubility, enrichment factors and isotopic composition of Zn and Cu in aerosols from the eastern tropical Atlantic Ocean are investigated in order to evaluate the utility of Zn and Cu isotope ratios as source tracers of natural and anthropogenic aerosols. Our goal is to better constrain the sources of aerosols and the input fluxes of Zn and Cu to the ocean in this region.

2 Methods

2.1 Samples and Study area

Eleven aerosol samples were collected in February-March 2011 during the GEOTRACES GA06 cruise in the eastern tropical Atlantic, between -7 ºN and 17 ºN (Fig. 1). Pre-cleaned Whatman 41 cellulose fibre

filters were used to collect the samples by high volume sampling ($\sim 1 \text{ m}^3 \text{ min}^{-1}$), when the wind direction ensured that the ship's exhaust emissions did not cause contamination. Eight of the eleven samples were collected in or very near a North African dust plume, which was situated between approximately 4 and 13 °N (Bridgestock et al., 2016). Air mass back trajectories (AMBT) reveal that these eight samples originated from North Africa (denoted NA), while the three more southerly samples (ISO-14, ISO-16, ISO-19) did not encounter land in the five days prior to collection (denoted Oceanic – OC; Fig. S1; Bridgestock et al., 2016; 2017).

Near the equator, rapidly rising, humid air creates the low-pressure belt of the inter-tropical convergence zone (ITCZ), which causes intense precipitation of about 2000 mm yr^{-1} (Helmers and Schrems, 1995). At the time of sampling, the ITCZ was situated at approximately 1 ºN (Schlosser et al., 2014). The large volume of rain scavenges atmospheric particles and, therefore, wet deposition dominates the supply of trace metals to the surface ocean in this region of the tropical Atlantic (Church et al., 1990; Helmers and Schrems, 1995). Trade winds transport large quantities of Saharan and Sahel dust to the sampling locations (Helmers and Schrems, 1995; Goudie and Middleton, 2001). However, southward transport of desert dust in the atmosphere is effectively shielded by particle scavenging in the ITCZ (Schlosser et al., 2014).

2.2 Materials and Methods

Sample preparation was carried out in ISO class 4 laminar flow hoods in an ISO 6 clean room at Imperial College London using acid-cleaned Savillex PFA beakers. The acids used (HCl, HNO_3, HF) were distilled in quartz or Teflon stills whilst concentrated optima grade H_2O_2 and $HClO_4$ were purchased from Fisher Scientific. The purified water used for diluting and cleaning procedures was from a Milli-Q water purification system (Merck Millipore; resistivity ~ 18.2 MΩ cm).

The digestion and leaching of the filters have been described previously (Bridgestock et al., 2016). Briefly, the filter papers were divided into two portions; one portion underwent a total digestion, which

involved additions of 15.6 M HNO_3, 9.8 M H_2O_2, 11.6 M $HClO_4$, 28 M HF, and 6 M HCl. The other portion

underwent leaching with 1.1 M ammonium acetate (pH 4.7). This leaching procedure has been used

extensively to investigate the labile fraction of Fe and other trace elements in marine aerosols (e.g.,

Bridgestock et al., 2016; Jickells et al., 2016). However, the relationship between trace element

dissolution in this medium and in seawater is unclear (Baker et al., 2016; Meskhidze et al., 2019), with

lower solubility in seawater (due to higher pH) probably offset by strong organic complexation (Campos

and van den Berg, 1994; Ellwood and van den Berg, 2000; Buck et al., 2012). Elemental concentrations

were measured using inductively coupled plasma mass spectroscopy (ICP-MS) and inductively coupled

plasma atomic emission spectroscopy (ICP-AES) at the Natural History Museum, London (Bridgestock et

al., 2016; 2017).

Sample solution aliquots for Zn and Cu isotope measurements were spiked with a ^{64}Zn-^{67}Zn double spike

to achieve a molar ratio of spike to sample-derived natural Zn (S/N) of close to 1.2 (Arnold et al., 2010;

Bridgestock et al., 2014). After double spike equilibration the samples were converted to chloride form

and dissolved in 7 M HCl + trace H_2O_2. Zinc and Cu were separated from the matrix and each other using

anion-exchange chromatography, following previously published methods (Maréchal, Télouk and

Albarède, 1999; Archer and Vance, 2004; Little et al., 2014a). Once separated, Zn underwent an

additional, smaller clean-up column (Bridgestock et al., 2014) and Cu two further duplicate column

passes (Little et al., 2014a, 2019).

Further, samples of Arizona Test Dust (ATD; Powdered Technology; Vanderstraeten et al., 2020) were

digested and leached using similar procedures. Briefly, ~20 mg samples of ATD were digested in a 3:1

mixture of concentrated 28 M HF: 15.6 M HNO_3, ultrasonicated and refluxed at 140 °C for 24 h. The

solutions were then evaporated to incipient dryness and taken up in 1 mL 15.6 M HNO_3 for refluxing at

120 °C overnight. The resulting solutions were dried and treated twice more with 15.6 M HNO_3. A

further three aliquots of ~20 mg of ATD were leached by immersion and agitation (5 x 2 min), in ~5 mL

of a 1.1 M ammonium acetate solution at pH 4.7 (prepared from 13.75 mL 17 M acetic acid, 9 mL 18.1 M

aqueous NH_3, MQ water) and the supernatant separated by centrifugation (4400 rpm, 10 min). The final

products were converted to chloride form and processed by ion exchange chemistry for the separation

of Zn and Cu in the same manner as the aerosol filter solutions. Finally, the USGS reference materials

BIR-1 (a basalt) and Nod-P1 (a Fe-Mn nodule) were digested and purified using the same methods to

verify the accuracy of the total procedure.

2.3 Zinc and Cu isotope compositions

Prior to isotope ratio analysis, Cu samples were dissolved in 1 mL ~5.6 M HNO_3 and 0.1 mL ~10 M H_2O_2

and refluxed at 180 °C overnight and Zn samples were treated with ~300 μL 15.6 M HNO_3. These

oxidation steps are designed to remove organics introduced by the resin. Each sample was then

dissolved in 2% HNO_3 to ~100 ppb total Zn and total Cu concentrations for isotopic analysis.

Zinc isotope compositions were measured using a Nu Plasma HR multi-collector inductively coupled

plasma mass spectrometer (MC-ICP-MS). The samples were introduced via either an Aridus II or DSN-

100 desolvating nebuliser system and a glass expansion Micromist nebuliser (uptake rate ~100 μL min^{-1}).

The MC-ICP-MS was operated in low resolution mode and each day the instrumental parameters were

adjusted to optimise the sensitivity, typically ~100 V ppm^{-1} for Zn. The Faraday cups were equipped with

10^{11} Ω resistors and simultaneously collected the ion beams of ^{64}Zn, ^{66}Zn, ^{67}Zn, ^{68}Zn, ^{62}Ni, $^{137}Ba^{2+}$. Prior to

each measurement (of 3 blocks of 20 x 5 s integrations), an analysis of 2% HNO_3 (20 x 5 s integrations)

was performed. The 2% HNO_3 acid blank 'background' measurement was subtracted from the sample

and standard results (Little et al., 2019).

Instrumental mass bias was corrected for the isotope ratios of Zn by the double spike technique outlined

in Arnold et al. (2010) and Bridgestock et al. (2014). The data was processed offline, including

interference corrections, following the iterative instrumental fractionation correction procedure

described by Siebert, Nägler and Kramers (2001). The isobaric interferences from ^{64}Ni and $^{(136, 134, 132)}$Ba^{2+} were accounted for by monitoring ^{62}Ni and ^{137}Ba^{2+} respectively; the interference corrections were nearly negligible with ^{64}Ni/^{64}Zn, ^{132}Ba^{2+}/^{66}Zn, ^{134}Ba^{2+}/^{67}Zn and ^{136}Ba^{2+}/^{68}Zn ratios for samples of typically less than 1x10^{-5} for samples. The Zn isotope compositions of samples were determined relative to bracketing runs of IRMM-3702 Zn standard solutions, which had total Zn concentrations and S/N ratios matched to within 10% of the samples and are reported in δ notation:

$$\delta^{66}Zn = \left(\left(\frac{\left(^{66}Zn \middle/ ^{64}Zn \right)_{sample}}{\left(^{66}Zn \middle/ ^{64}Zn \right)_{IRMM-3702}} \right) - 1 \right) \times 1000 \qquad 1$$

All Zn isotope data are reported relative to the JMC Zn isotope standard. As the isotopic analyses were conducted relative to IRMM-3702 Zn, a correction of +0.30 ‰ was applied following the recommendation of Moynier et al. (2017) and Archer et al. (2017). Repeated analyses of the in-house London Zn isotope standard on multiple days of analysis yielded δ^{66}Zn$_{JMC}$ = +0.14 ± 0.08 (n = 23, 2 SD; Table S1).

All Cu isotope analyses were performed on a Nu Plasma II MC-ICP-MS at Imperial College London. Samples were introduced using a Peltier glass spray chamber (5 °C) coupled to a glass expansion Micromist nebuliser (uptake rate ~100 μL min^{-1}). The instrument was operated in low resolution mode with an average sensitivity (total Cu beam) of ~25 V ppm^{-1}. In order to correct for instrumental mass bias, samples were doped with Ni, as described by Larner et al. (2011) and Little et al. (2019), to achieve a 3:1 Ni:Cu (± 20%) ratio for samples and standard solutions. Tests showed that a 20% discrepancy in Ni:Cu ratio had no impact on the corrected Cu isotope data. Each sample and standard measurement (of 60 x 5 s integrations) was preceded by a 'background' run (20 x 5 s integrations) of a 2% HNO$_3$ blank

solution; the background signals were subsequently subtracted from the Cu (and Ni) ion beams measured in the sample and standard runs (Little et al., 2019). This yielded raw measured $^{65}Cu/^{63}Cu$ ratios, which were corrected online for the instrumental mass bias using the $^{62}Ni/^{60}Ni$ ratio and the exponential law. The $\delta^{65}Cu_{NIST}$ values of the samples were determined relative to bracketing runs of the ERM-AE633 Cu standard, as detailed by Nielsen et al. (2004) for Tl and Pb and Larner et al. (2011) for Cu and Ni.

$$\delta^{65}Cu = \left(\left(\frac{\left(^{65}Cu\big/_{63}Cu\right)_{Sample}}{\left(^{65}Cu\big/_{63}Cu\right)_{ERM-AE633}}\right) - 1\right) \times 1000 \qquad 2$$

All Cu isotope data are reported relative to NIST SRM 976 Cu. As the $\delta^{65}Cu$ values were acquired relative to ERM-AE633 Cu, these results were corrected by -0.01 ‰ following the recommendation of Moynier et al. (2017). Multiple analyses of the secondary Romil Cu isotope standard yielded $\delta^{65}Cu_{NIST}$ = +0.24 ± 0.08 ‰ (n = 13, 2 SD; Table S2).

The purified Cu fractions from the anion exchange separation must achieve a (near-) perfect yield, as Cu isotope fractionation may occur on the resin columns; previous work has shown that the applied procedure routinely provides essentially perfect (103%) Cu yields (Little et al., 2014). Whilst Cu yields could not be determined for the samples of this study (due to the unknown Cu concentrations), the mean Cu yield for column-processed reference materials was 109 ± 20% (n = 9, 2 SD).

All uncertainties on isotopic compositions are hereafter based on the long-term 2 SD reproducibility of the Romil Cu and London Zn secondary standards, both 0.08 ‰.

3 Results

3.1 Quality Control

The mean total procedural blank for Zn, including the total digestion and leaching procedures and anion exchange chromatography procedures, was 3.8 ng (n = 5, 0.5–9.1 ng), less than 4% of the Zn content of the smallest sample. Total procedural blanks for Cu were 0.18 ng (n = 4, 0.06–0.35 ng), less than 1% of the Cu content of the smallest sample.

Three types of filter blank were analysed to examine the blank associated with the sample collection procedure. They can be thought of as incrementally progressing through the sampling process (as described in Baker et al., 2006 and in the Supplementary Text). Briefly, 'filter blanks' undergo the filter pre-cleaning procedure. A 'cassette blank' is pre-cleaned and placed inside the air sampling unit without exposure to the air. Finally, 'exposure blanks' are pre-cleaned, placed in the sampling unit and exposed to the air, but without the sampler unit (i.e., the motor) turned on. Filters representing each of the three types of sampling blank underwent the same leaching and total digestion procedures as the samples. Zinc concentrations in the total digest exposure blanks exceed Zn concentrations in several of the real samples and are typically considered an overestimation of the sampling blank (discussed in Baker et al., 2006). For further discussion of the representativeness of exposure blanks, please see the Supplementary Text. Our best estimate for the total digest Zn blank is, therefore, the mean of the filter blank and cassette blank, giving 512 ng per filter (n = 2, 459 and 565 ng) and an average Zn isotope composition of +0.10 ‰ (n = 2, +0.04 and +0.16 ‰; Table 1). The cassette blank leachate solution yielded 2123 ng of Zn, far higher than the corresponding total digest value of 565 ng (Table 1). This blank is a clear outlier and is omitted. The remaining three leachate solutions (one filter blank, two exposure blanks) had much smaller quantities of Zn, at 574 ng, 161 ng and 232 ng respectively (Table 1). We take the filter blank as a conservative estimate of the leachate Zn blank (574 ng, $\delta^{66}Zn$ = +0.02 ‰). The mean

digest and leachate Zn blank values (512 and 574 ng per filter, respectively) were used to blank subtract the total digest and leachate concentration data presented in Table 2. Respective blank contributions are presented in Table S3. Blank-corrected sample Zn isotope compositions (Table S3) are all within analytical uncertainty (± 0.08 ‰) of uncorrected values, and are therefore considered insignificant, and Zn isotope compositions are reported uncorrected in Table 2. Note, the ISO-8 leachate sample has the largest blank contribution, at 52%, because this sample contains the lowest Zn concentration (a factor three lower than any other sample); therefore, the δ^{66}Zn value for the ISO-8 leachate should be considered with caution.

For Cu, sampling blanks were estimated as the average of two filter blanks, an exposure blank and a cassette blank, yielding a value of 66 ng per filter for the total digest (range 37 to 122 ng per filter; Table 1) and 27 ng per filter for the leachate (range 15 to 40 ng per filter; Table 1). For all aerosol samples, other than ISO-11 total digest and leachate, the blank contributions are less than 6% (with an average of 2%, Table S3). The ISO-11 total digest and leachate samples have blank contributions of 12% and 18%, respectively. Aerosol sample Cu concentrations are blank-corrected in Table 2. The Cu concentrations of filter blanks were not analysed, so blank corrections were not possible for the isotope data; nevertheless, any blank correction is expected to be insignificant given the minor sampling blank contribution.

3.2 Atmospheric Zn and Cu concentrations and aerosol isotopic compositions

Atmospheric concentrations (ng metal/m^3 of air) were calculated using the mass measured on the filter (ng), the exposure time (min) and the sampling rate (1 m^3 min^{-1}). Atmospheric Zn concentrations in the total digests range from 0.78 to 10.03 ng m^{-3} and 0.29 to 4.50 ng m^{-3} in the leachates. Atmospheric Cu concentrations in the total digests range from 0.28 to 4.23 ng m^{-3} and 0.11 to 1.40 ng m^{-3} in the leachates (Table 2, Figs. 2, 3).

Total digest δ^{66}Zn values range from -0.02 to +0.41 ‰ and δ^{65}Cu values exhibit a larger variability from -0.34 to +0.26 ‰ (Table 2, Figs. 2, 3). Leachate samples present a range in Zn isotope compositions of 0.00 to +0.25 ‰ and the two leachate Cu isotope compositions are +0.03 and +0.27 ‰ (Table 2, Figs. 2, 3).

The leachate and total digest aerosol isotopic compositions for both Zn and Cu are isotopically indistinguishable. The mean δ^{66}Zn values for the leachates and total digests are +0.15 ± 0.16 ‰ (n = 7) and +0.17 ± 0.22 ‰ (n = 11) respectively. The average isotopic composition of Cu in the total digests and leachates are also similar, at +0.07 ± 0.39 ‰ (n = 9) for the total digests and +0.27 ‰ and +0.03 ‰ for the leachates, but as only two leachate samples were analysed the δ^{65}Cu comparison is less robust. Systematic isotopic differences are observed between the total digest and leachate Zn and Cu isotope compositions for the Arizona Test Dust (ATD; Table 3; Vanderstraeten et al., 2020). Total digests yield an average δ^{66}Zn value of +0.29 ‰ (n = 3, range +0.21 to +0.33 ‰) and δ^{65}Cu value of +0.21 ‰ (n = 3, range +0.19 to +0.22 ‰), Table S4 reports the ATD data relative to previously published bulk values, suggesting some heterogeneity between batches. By comparison to total digest values, ATD leachates are isotopically heavy, with an average δ^{66}Zn value of +0.50 ‰ (n = 3, range +0.47 to +0.52 ‰) and δ^{65}Cu of +0.62 ‰ (n = 3, range +0.58 to +0.65 ‰). Explaining this phenomenon would require detailed compositional analysis of ATD. We note, however, that both Zn and Cu in ATD are poorly soluble, with release of only 16% and 8‰, respectively of the total elemental budgets (eqn. 4, section 4.1.1). The low solubility and the isotopically heavy leachates suggest that a minor labile phase is solubilised by the leaching procedure, while the major part of the ATD Zn and Cu budgets are present in silicate/ oxide minerals, which are only attacked by the total digestion procedure.

4 Discussion

4.1 Examining the extent of anthropogenic metal contributions to tropical Atlantic aerosols

4.1.1 Enrichment factors and fractional solubility

Enrichment factors (EF) are a first-order means to assess the extent of non-crustal inputs to an aerosol sample (Zoller et al., 1974). The studied element X to Al ratio in the sample is divided by the same ratio measured in upper continental crust (UCC; values from Rudnick and Gao, 2003).

$$EF = \frac{(\frac{X}{Al})_{Aerosol}}{(\frac{X}{Al})_{UCC}} \quad 3$$

The trace element of interest (X) is compared to Al because the vast majority of Al in the atmosphere is derived from crustal sources (Lantzy and Mackenzie, 1979). An enrichment factor greater than 1 signifies enrichment with non-crustal sources. However, due to uncertainty in how well the chosen UCC reference ratio represents that of the mineral dust in the sample, a value >10 is generally considered to confidently indicate a non-crustal source (e.g., Lantzy and Mackenzie, 1979; Chester, 1993; Gao et al., 2002; Tositti et al., 2014; Ochoa Gonzalez et al., 2016). Uncertainties in EF values were calculated by error propagation using the mean filter blank concentration values of Al, Zn and Cu as the error on their respective concentrations, see Equation S2.

Of the eight aerosol samples that were collected in or in close proximity to the dust plume, which originated from North Africa (NA; Fig. 1), the majority have near crustal elemental compositions, indicated by low Zn and Cu enrichment factors of <10 (Fig. 4, Table 4). These samples likely contain a large mineral dust contribution. The exception is ISO-25, which has elevated Zn and Cu EF values of 13 and 11, respectively (Fig. 4, Table 4). ISO-25 was sampled between latitudes 11.45 and 17.42 °N, partially in and partially out of the dust plume (Baker et al., 2020), suggesting that aerosols north of the plume contain a more significant anthropogenic contribution.

The three oceanic (OC) samples, ISO-14, -16 and -19, are more enriched in both Zn and Cu than the NA samples, (Fig. 4, Table 4). This enrichment suggests a larger anthropogenic contribution to aerosols collected south of the dust plume and, particularly, south of the ITCZ. Intense precipitation in the region influenced by the ITCZ (estimated at 2000 mm yr^{-1}; Helmers and Schrems, 1995) scavenges atmospheric particles from air masses moving in a southerly direction (Schlosser et al., 2014), limiting the amount of mineral dust from the Sahara reaching ISO-14,-16 and -19. Further, based on the negative linear relationships in $\log_{10}$-$\log_{10}$ graphs of EF values for Zn, Pb and Cd versus atmospheric Al concentrations for the aerosols of this study, Bridgestock et al. (2017) infer a constant anthropogenic background, which is mixed with pulses of Saharan dust (Chester, 1993). The same effect is observed here for Cu (Fig. 5). The EF values determined for both Zn and Cu using alternative elements for normalisation, e.g., Sc, Ti, Th, display the same systematics as the results obtained with Al normalisation (Table S5). Furthermore, the close correlation between the concentrations of Zn and Cu (Fig. S2) for the total digest aerosol samples implies that the trace metals originate from similar sources.

The predominant source of Na is from the ocean (Tsyro et al., 2011) making it an effective tracer for sea spray contributions to the aerosol samples (White, 2008). The sea spray contribution was assessed by assuming all the Na present in the aerosols derived from seawater and utilising Na, Zn and Cu seawater concentrations of 10.76 g kg^{-1}, 0.1 nmol kg^{-1} and 0.75 nmol kg^{-1}, respectively (Millero et al., 2008). The resultant contributions are a fraction of a percent of the total Zn and Cu present in the aerosols, and thus sea spray is deemed a negligible source for Zn and Cu in these samples.

The atmospheric supply of soluble trace metals to the surface ocean reflects the aerosol flux, metal concentrations, and fractional solubility. The mode of aerosol deposition, either wet or dry, is also partially controlled by solubility, as hygroscopic particles are more likely to be incorporated into rainfall. The predominant mode of deposition varies strongly in the eastern tropical North Atlantic driven primarily by the seasonally-variable position of the ITCZ (Church et al., 1990; Helmers and Schrems,

1995; Powell et al., 2015). During the GA06 cruise, rainfall associated with the ITCZ was observed

between 5.0 °S and 3.4 °N, meaning wet deposition was likely to be the dominant mode within this

zone, while dry deposition was more important in the dusty airmasses further north (Powell et al.,

2015). Trace metal solubility in wet deposition appears to be higher than in dry deposition (Powell et al.,

2015). The pH of the leachate procedure used in this study (~4.7) is closer to that of rainwater than

surface seawater (~8.1), but similar procedures have been used to estimate the bioavailable Fe content

of particulate matter in seawater (Bruland et al., 2001). The fractional solubility of each aerosol sample

is calculated as follows:

$$Fractional\ solubility\ (\%) = \frac{[leachate]}{[total\ digest]} \times 100 \qquad 4$$

Error propagation based on the

uncertainties of the atmospheric

concentrations is used to calculate the uncertainty on the fractional solubilities (see Equation S3). The

calculations yield a large range in fractional solubilities for both Zn (7–136%) and Cu (7–84%) (Table 4).

Three Zn samples have solubilities greater than 100%; i.e., the Zn concentrations of the leachate

solutions exceeded those of the total digest. Comparison with other elements (Al, Nd, Sc), suggests

these high solubilities likely reflect sample heterogeneity rather than contamination, with the possible

exception of ISO-11, because elevated solubilities are also observed for these other, less contamination

prone elements (Fig. S3).

The large range in fractional solubilities likely reflects the variable contributions of natural versus

anthropogenic Zn and Cu sources (e.g., Mahowald et al., 2018; Shelley et al., 2018). The solubilities of

both elements from mineral dust are typically low. For example, Zn solubility from Saharan loess

collected in Cape Verde was reported to be 11% and 16% in acidified MQ water (pH 4.7) and seawater,

respectively (Desboeufs et al., 2005; Thuróczy et al., 2010). Copper solubility of 27% was determined for

Saharan dust from Cape Verde in acidified MQ water (pH 4.7), while for Saharan dust from Bermuda it

was 1-7% in deionized water at pH 5.5 (Desboeufs et al., 2005; Sholkovitz et al., 2010). By contrast,

elemental solubilities reported for anthropogenic aerosols are generally higher. For example, Sholkovitz

et al. (2010) found Cu solubilities of up to 100% for anthropogenic aerosols and Desboeufs et al. (2005)

measured Zn and Cu solubilities of 99% and 98%, respectively, for fly ash from heavy fuel combustion.

Therefore, a high fractional solubility for an aerosol-bound metal is an indicator of significant

anthropogenic content (Mahowald et al., 2018). The majority of the fractional solubilities determined

for Zn and Cu in the aerosols of this study exceed the published values for Saharan dust, suggesting that

they all contain some anthropogenic particles. The samples from outside of the North African dust

plume with high enrichment factors (oceanic samples and ISO-25) have larger fractional solubilities,

exceeding 64% for Zn and Cu, than the samples collected within the dust plume (average for Zn: 52 ±

72%, n = 7, 2 SD and average for Cu: 31 ± 50%, n = 7, 2 SD).

To conclude, high enrichment factors and fractional solubilities indicate a significant anthropogenic

component in the trace metal budgets of, in particular, the oceanic aerosol samples, collected south of

the ITCZ. In the following, the Cu or Zn isotope compositions of the aerosols are examined to constrain

the origins of the anthropogenic contribution.

4.1.2 Examining the extent of an anthropogenic contribution using Cu isotope compositions

The mean total digest δ^{65}Cu value, of +0.07 ± 0.39 ‰ (n = 9), is congruent with the lithogenic Cu isotope

composition, at +0.08 ± 0.40 ‰ (n = 42; Moynier et al., 2017). Furthermore, Dong et al. (2013) and Little

et al. (2014) report δ^{65}Cu values of -0.08 ± 0.10 ‰ (n = 6) and 0.00 ± 0.36 ‰ (n = 6) respectively for

leached Atlantic aerosols, similar to those of this study. It is notable, however, that lithogenic and

aerosol Cu isotope compositions are considerably more variable than the isotopic compositions of

chemically similar elements, such as Zn and Cd (this study; Bridgestock et al., 2017). For example, Dong

et al. (2013) report a relatively low δ^{65}Cu value of -0.24 ± 0.11 ‰ (n = 6) for a homogenised mineral dust

sample from the Sahel region, and Takano et al. (2020) report a wide range of Cu isotope compositions

from -0.33 to +0.83 ‰ for aerosols from the North Pacific Ocean. Furthermore, no systematic

relationship is observed for the aerosols between Cu isotope compositions and enrichment factors (Figure S4). In detail, ISO-14 has the highest EF coupled with a relatively heavy Cu isotope composition of +0.24 ‰, whilst the sample with the most positive δ^{65}Cu value (ISO-23, +0.26 ‰) has a low EF of 4.4. Sample ISO-11 has a very low δ^{65}Cu value of -0.34 ‰, lower than the compiled values for Saharan mineral dust (-0.24 to +0.09 ‰, n = 5; Schleicher et al., 2020), and may thus record anthropogenic Cu input. The dominant anthropogenic sources of Cu are from non-ferrous metal production, fossil fuel combustion, and non-exhaust vehicular emissions (specifically brakes; Pacyna and Pacyna, 2001; Hulskotte et al., 2007; Dong et al., 2013). Anthropogenic sources have variable Cu isotope compositions, reviewed by Schleicher et al. (2020). For example, brake pads are isotopically heavier than lithogenic Cu (+0.3 to +0.7‰; Dong et al., 2017), while coal displays light Cu isotope compositions, from -1.35 ‰ to -0.35 ‰ (Novak et al., 2016). Copper isotope fractionation during smelting activities appears to be negligible, such that the output waste has similar δ^{65}Cu values to the feed material, which can be isotopically light (e.g., δ^{65}Cu = -0.5 ‰; Mihaljevič et al., 2018).

In conclusion, both anthropogenic and natural Cu sources are isotopically variable (Schleicher et al., 2020). Hence, while anthropogenic activities are undoubtedly increasing the quantity of Cu deposited into the ocean, with consequences for marine ecosystems (section 4.2.1), conclusive fingerprinting of sources using Cu isotopes is not yet feasible.

4.1.3 Examining the extent of an anthropogenic contribution using Zn isotope compositions

In contrast to Cu, lithogenic Zn isotope compositions are relatively homogeneous (at about +0.3 ‰), and the majority of potential atmospheric contaminant phases are isotopically lighter than the lithogenic Zn isotope signature (e.g., John et al., 2007; Mattielli et al., 2009). Next, the utility of Zn isotope compositions as a tracer of anthropogenic contributions to tropical Atlantic aerosols is evaluated.

The principal anthropogenic source of atmospheric Zn is metal production in non-ferrous refineries (Nriagu, 1979; Pacyna and Pacyna, 2001; Shiel et al., 2010). Pyrometallurgical processes fractionate Zn

isotopes (John et al., 2007; Shiel et al., 2010; Yin et al., 2016), because temperatures during roasting and grilling exceed the boiling point of Zn (907 °C) and partial volatilisation and condensation can induce kinetic isotope fractionation via Rayleigh distillation (Sivry et al., 2008; Shiel et al., 2010). Mattielli et al. (2009) measured Zn isotope ratios for particles collected both inside a Pb-Zn refinery and on deposition plates within a 5 km radius, calculating a mean δ^{66}Zn value for refinery emissions of -0.21 ‰ (range: -0.73 to +0.21 ‰; Mattielli et al., 2009). Industrial emissions with light Zn isotope compositions have been further corroborated by aerosols from an industrial region near São Paulo, with a mean δ^{66}Zn of -0.33 ± 0.34 ‰ (n = 12) (Souto-Oliveira et al., 2018).

Aside from non-ferrous refinery emissions there are several additional anthropogenic Zn sources to the atmosphere (Fig. 6; recently reviewed by Schleicher et al., 2020). In the context of the eastern tropical Atlantic, relevant sources are likely those that generate fine particles with long residence times in the atmosphere, which includes all types of combustion emissions (e.g., fossil fuel burning and fires; Bauer et al., 2004; Mahowald et al., 2018). The majority of combustion emissions have low δ^{66}Zn values of -0.73 to +0.21 ‰ (Schleicher et al., 2020), whilst burning of coal can create fly ash with much heavier compositions (δ^{66}Zn ≈ +0.8 ‰) due to the isotopically heavy coal feed material (Ochoa Gonzalez and Weiss, 2015).

Traffic emissions are a significant anthropogenic source of atmospheric Zn (Souto-Oliveira et al., 2018). Though the Atlantic sampling location is far from urban environments, the samples of this study were collected in proximity to fishing localities and high-traffic shipping lanes frequented by tankers as well as container and passenger ships, which travel from the South American east coast to the Mediterranean (Johansson et al., 2017). Global shipping activity has increased four-fold since the 1950s, and currently the particulate matter emitted by ships constitutes more than 10% of total European small particle emissions (<2.5 μm) (Wan et al., 2016). Turner et al. (2017) report very high average Zn and Cu concentrations for waters discharged from ships by open loop scrubbers (at 136 and 60 μg L^{-1},

respectively). Furthermore, measurements of engine emissions from large ocean-going vessels in operation at sea reveal ranges in Zn concentrations of 0.5–5 g/ h, depending on engine load (Agrawal et al., 2008a; Agrawal et al., 2008b). To our knowledge, no Zn isotope data for shipping emissions have been published to date. However, road dust collected from London and São Paulo has a mean δ^{66}Zn value of +0.17 ± 0.19 ‰ (n = 13), and the Zn isotope compositions of aerosols collected in tunnels are significantly lighter than road dust, by ~0.3 ‰ (Souto-Oliveira et al., 2019). These tunnel-collected aerosols were inferred to be isotopically light because they encompass all vehicle emissions, including isotopically light particles from fuel combustion (Souto-Oliveira et al., 2019).

Lastly, biomass burning in Africa is a likely source of aerosols to the Atlantic Ocean, because smoke particles mix and travel effectively with, but also independently of, desert dust (Heinold et al., 2011). Biomass burning is prevalent in West Africa (Van Der Werf et al., 2010). Smoke from the fires reaches high altitudes and injects the particles into the mixing layer (Labonne et al., 2007), which propagates westwards to the Atlantic (Adams et al., 2012). Furthermore, Zn is enriched in pyrogenic emissions, and fine particles in air that has been impacted by biomass burning are highly soluble (Maenhaut et al., 1996; Baker and Jickells, 2017). To our knowledge, no Zn isotope data are available for aerosols produced by biomass burning.

To summarise, the δ^{66}Zn values of various anthropogenic emissions span a wide range, from -0.73 ‰ (Pb-Zn refinery; Mattielli et al., 2009) to +1.9 ‰ (coal fly ash; Ochoa Gonzalez and Weiss, 2015). However, anthropogenically sourced Zn is generally isotopically lighter than Zn from natural sources, with anthropogenic δ^{66}Zn values predominantly between -0.4 and +0.2 ‰ (Fig. 6).

As discussed, the Atlantic aerosol samples collected outside of the North African dust plume (Oceanic samples, plus ISO-25) generally display the highest Zn enrichment factors and higher fractional solubilities than the North African samples collected within the plume, consistent with a larger anthropogenic component in the former. Therefore, based on mixing between mineral dust (with δ^{66}Zn

≈ +0.3 ‰; Schleicher et al., 2020) and one or several anthropogenic sources that are isotopically light, aerosol samples from within the North African dust plume should be isotopically heavier than those from outside the plume. However, the Zn isotope compositions of the dust plume samples, at +0.18 ± 0.27 ‰ (n = 7), are indistinguishable from the samples collected outside of the plume, at +0.16 ± 0.13 ‰ (n = 4). Nevertheless, all aerosol samples, except for the total digest of ISO-8 (+0.41 ‰), which has the lowest fractional solubility (7%), are isotopically lighter than mineral dust. Hence, we suggest that the Zn isotope compositions of almost all aerosol samples from the eastern tropical Atlantic, not just those from outside the dust plume, are likely impacted by anthropogenic Zn contributions.

Quantification of the anthropogenic contribution to the aerosols can be attempted by coupling the Zn isotope data with published Pb isotope compositions for the same samples (Bridgestock et al., 2016; Fig. 7). Lead isotopes are a well-established tracer of anthropogenic emissions (e.g., Patterson and Settle, 1987; Reuer and Weiss, 2002; Bridgestock et al., 2016). A cross plot of Zn and Pb isotope compositions (Fig. 7) confirms that all the aerosol samples contain a substantial anthropogenic contribution, as the samples plot on mixing lines between a lithogenic component (Bridgestock, 2015 and references therein; Moynier et al., 2017) and an endmember defined by Pb-Zn refinery emissions (Cloquet et al., 2006b; Mattielli et al., 2009).

The mean Zn and Pb concentrations of the upper continental crust are relatively well-established, at 67 and 17 µg g^{-1}, respectively (Rudnick and Gao, 2003), defining a Zn/Pb ratio of 3.94 for the lithogenic endmember. Given this, the mixing relationships shown by the data can be applied to constrain the Zn:Pb ratio of the anthropogenic component.

Figure 7 displays three mixing lines, denoted as a, b and c, which account for Zn-Pb isotope systematics of the aerosols. No concentration influence is applied for either endmember in curve 'a'. The other two mixing curves, 'b' and 'c', both employ a lithogenic component with Zn/Pb = 3.94 and assume anthropogenic endmembers with Zn/Pb ratios of 1 and 0.09 respectively, which are in accord with

average Zn and Pb concentrations reported for refinery emissions by Mattielli et al. (2009) and Cloquet

et al. (2006b). A lower anthropogenic Zn/Pb ratio compared to lithogenic Zn/Pb is expected because Pb

is more volatile than Zn. Mixing line 'b' encompasses the majority of our data (Fig. 7), suggesting that

the anthropogenic source (or combination of sources) is characterised by a Zn/Pb ratio of approximately

1. Given these assumed endmember Zn/Pb ratios (of 3.94 and 1 respectively), the position of the

samples in Fig. 7 relative to mixing line 'b' furthermore implies that 60–90% of the Zn and Pb in the

aerosols is of lithogenic origin. However, this model is not a unique solution to explain the aerosol Zn-Pb

isotope compositions. In particular, improved constraints on the local anthropogenic sources of Zn and

Pb (e.g., from shipping) are desirable to enable more robust quantification of the anthropogenic

contributions.

Overall, Zn isotope compositions appear to be an effective indicator for an anthropogenic contribution

to the Zn inventory of aerosols. Our results also suggest that coupled Zn and Pb isotope data for aerosols

have the potential to provide constraints on the sources of anthropogenic metal emissions to the

atmosphere.

4.2 Aerosols in an oceanic context

4.2.1 Links between aerosol solubility and Cu toxicity
As discussed, a key control on the solubility of aerosols is the extent of the anthropogenic contribution.

Increasing emissions of anthropogenic aerosols will, therefore, lead to larger fluxes of generally volatile

elements, which are enriched in industrial and urban emission sources, to the ocean (Mahowald et al.,

2018). Copper emissions to the atmosphere have increased by about a factor of x15 over the past 200

years (Hong et al., 1996) and, in certain regions (e.g., West Pacific), dry deposition of Cu has increased 4-

fold from preindustrial levels (Paytan et al., 2009). Although Cu is an essential nutrient for

phytoplankton, elevated levels of free Cu(II) are a primary toxicant (e.g., Sunda, 1976) and toxic Cu

concentrations in surface waters (e.g., Bay of Bengal) have been modelled by Paytan et al. (2009) and

Jordi et al. (2012). In general, higher marine Cu concentrations may be a contributing factor to the declining phytoplankton biomass inferred for the global ocean over the past century (Boyce et al., 2010). However, the Cu toxicity threshold is species dependent. Whilst the reproduction rates of cyanobacteria (e.g., *Synechococcus bacillaris*) are reduced at Cu^{2+} concentrations of 10^{-12} M, diatoms such as *Thalassiosira oceanica* are able to withstand much higher cupric ion activities of up to 10^{-9} M (Brand et al., 1986). Phytoplankton combat the toxicity of Cu(II) by releasing strong organic ligands to enhance extracellular complexation reactions (e.g., Moffett and Brand, 1996). This organic complexation reduces Cu toxicity for the most Cu sensitive prokaryotes, whilst the ligand-bound Cu remains bioavailable for some eukaryotic phytoplankton (e.g., Quigg, Reinfelder and Fisher, 2006; Semeniuk *et al.*, 2015). Nevertheless, the varying Cu(II) resistance of different phytoplankton species implies that the ecological diversity of marine regions is influenced by the ambient dissolved Cu concentrations (Gustavson and Wängberg, 1995).

Although the production of organic ligands can mitigate Cu toxicity, higher Cu concentrations can saturate Cu-binding ligands and exceed the toxicity threshold (Moffett et al., 1997). In the Mediterranean Sea, Jordi et al. (2012) estimated that Cu becomes toxic at a Cu deposition flux of 9.04 µg $m^{-2} d^{-1}$ (10^{-13} M), as higher fluxes have a detrimental impact on total chlorophyll concentrations. It is challenging to accurately estimate a mean Cu input flux to the eastern tropical Atlantic Ocean based on the aerosol data of this study. However, combining the maximum aerosol-based atmospheric Cu concentration (4.23 ng m^{-3}) with a deposition velocity of 0.02 m s^{-1} (Jordi et al., 2012) yields a maximum Cu deposition flux of 7.3 µg $m^{-2} d^{-1}$. This simple calculation implies that dry deposition of Cu in the eastern tropical Atlantic may not exceed the Cu toxicity threshold as estimated for the Mediterranean Sea, albeit that there are significant uncertainties in estimating the potential for variable aerosol Cu concentrations and deposition velocities. More work is needed to understand how these aspects, and the Cu toxicity threshold, vary for different ecological regimes, including the open ocean, and to

determine the impact of anthropogenic aerosols on the ecological composition of diverse oceanographic settings.

4.2.2 Aerosols: an isotopically light source of Zn to the surface ocean?

Isotopically light Zn isotope compositions are observed in many marine regions at sub-surface depths, between 0 and 300 m. This observation is well documented by δ^{66}Zn values as low as -1.08 ‰ in the North Atlantic (Conway and John, 2014) and -0.15 ‰ in the North East Pacific (Conway and John, 2015). While these signatures have been attributed to scavenging of isotopically heavy Zn by particles (e.g., John and Conway, 2014; Weber et al., 2018; Liao et al., 2020), recent studies have suggested that they may reflect inputs from an isotopically light, anthropogenic Zn source (Lemaitre et al., 2020; Liao et al., 2020). The importance of anthropogenic inputs to the oceanic internal Zn cycling is further supported by Liao et al. (2021) who measured relatively isotopically light δ^{66}Zn values (mean +0.12 ± 0.10 ‰, n = 18, 2 SD) in aerosols in the northern South China Sea attributed to anthropogenic sources.

The 2011 GEOTRACES GA03 cruise traversed the North Atlantic Ocean, passing near to the GA06 sampling locations of this study in the eastern tropical Atlantic. Conway and John (2014) reported δ^{66}Zn values of -0.15 ‰, -0.22 ‰ and -0.33 ‰ at depths of ~30 m for GA03 stations 12 (17.40 ºN, 24.50 ºW), 11 (17.35 ºN, 22.78 ºW) and 10 (17.35 ºN, 20.82 ºW), respectively (see Figure 1). These three stations are in close proximity to the sampling location of ISO-25 (+0.12 ‰). As such, aerosol samples analysed in this study, including ISO-25, are isotopically too heavy to be directly responsible for negative δ^{66}Zn that are observed in the sub-surface eastern tropical Atlantic Ocean. The data of this study also provide no evidence for Zn isotope fractionation during leaching of marine aerosols. However, the aerosols only characterise the input supplied by dry deposition, and they are therefore not wholly representative of the integrated atmospheric δ^{66}Zn input. Further work is required to evaluate the δ^{66}Zn values of wet versus dry deposition, and the potential for isotopic fractionation during partial solubilisation of aerosols

in seawater (i.e., at pH 8.1), or the potential for scavenging of Zn stimulated by aerosol deposition (Liao et al., 2020).

5 Conclusion

The atmospheric concentrations and isotopic compositions of Zn and Cu are reported for aerosol samples from the eastern tropical Atlantic Ocean. High fractional solubilities (typically >40% for Zn and >30% for Cu) and elemental enrichment factors (1.3–24 for Zn, and 1.1–23 for Cu) indicate significant anthropogenic contributions to the Zn and Cu budgets of the aerosols

Anthropogenic Cu in aerosols does not have a distinct Cu isotope signature. The maximum Cu inputs to the eastern tropical Atlantic Ocean that can be inferred from the aerosol concentrations do not exceed the toxicity threshold for phytoplankton that was previously reported for the Mediterranean Sea. Nevertheless, further work is required to better constrain the impact of atmospheric Cu inputs, particularly those supplied via wet deposition, on the ecological composition of the open ocean. With regard to Zn, tropical Atlantic Ocean aerosols are almost universally isotopically lighter than lithogenic sources. However, aerosol $\delta^{66}Zn$ values (+0.17 ± 0.22 ‰, n = 11, 2 SD) are too high to be directly responsible for the light Zn isotope compositions that have been observed for subsurface waters of this region. Nevertheless, they do indicate the presence of a significant anthropogenic atmospheric Zn component even in the strongly dust-dominated equatorial Atlantic region. This anthropogenic influence is evident from combined aerosol $\delta^{66}Zn$ and Pb isotope data, which show intermediate compositions between a lithogenic component and an anthropogenic endmember defined by Pb-Zn refinery emissions. To further characterise anthropogenic emissions, future studies should explore the Zn concentrations and isotope compositions of emissions from shipping and biomass burning. Our results demonstrate that Zn isotope compositions can be of utility for aerosol source tracing, such that marine regions in close proximity to intense anthropogenic activity are predicted to have a pronounced fingerprint with isotopically light Zn in the surface ocean.

Acknowledgements

References

Adams A. M., Prospero J. M. and Zhang C. (2012) CALIPSO-Derived three-dimensional structure of aerosol over the atlantic basin and adjacent continents. *J. Clim.* **25**, 6862–6879.

Agrawal H., Malloy Q. G. J., Welch W. A., Wayne Miller J. and Cocker D. R. (2008a) In-use gaseous and particulate matter emissions from a modern ocean going container vessel. *Atmos. Environ.* **42**, 5504–5510.

Agrawal H., Welch W. A., Miller J. W. and Cocker D. R. (2008b) Emission measurements from a crude oil tanker at sea. *Environ. Sci. Technol.* **42**, 7098–7103.

Archer C., Andersen M. B., Cloquet C., Conway T. M., Dong S., Ellwood M., Moore R., Nelson J., Rehkämper M., Rouxel O., Samanta M., Shin K. C., Sohrin Y., Takano S. and Wasylenki L. (2017) Inter-calibration of a proposed new primary reference standard AA-ETH Zn for zinc isotopic analysis. *J. Anal. At. Spectrom.* **32**, 415–419.

Arnold T., Schönbächler M., Rehkämper M., Dong S., Zhao F. J., Kirk G. J. D., Coles B. J. and Weiss D. J. (2010) Measurement of zinc stable isotope ratios in biogeochemical matrices by double-spike MC-ICPMS and determination of the isotope ratio pool available for plants from soil. *Anal. Bioanal. Chem.* **398**, 3115–3125.

Baconnais I., Rouxel O., Dulaquais G. and Boye M. (2019) Determination of the copper isotope composition of seawater revisited: A case study from the Mediterranean Sea. *Chem. Geol.* **511**, 465–480.

Baker A. R. and Jickells T. D. (2017) Atmospheric deposition of soluble trace elements along the Atlantic Meridional Transect (AMT). *Prog. Oceanogr.* **158**, 41–51.

Baker A. R., Jickells T. D., Witt M. and Linge K. L. (2006) Trends in the solubility of iron, aluminium, manganese and phosphorus in aerosol collected over the Atlantic Ocean. *Mar. Chem.* **98**, 43–58.

Baker, A.R., Landing, W.M., Bucciarelli, E., Cheize, M., Fietz, S., Hayes, C.T., Kadko, D., Morton, P.L., Rogan, N., Sarthou, G., Shelley, R.U., Shi, Z., Shiller, A.M. and Van Hulten, M.M.P. (2016) Trace element and isotope deposition across the air – sea interface: Progress and research needs. *Philos. Trans. A* **374**, 20160190.

Baker, A. R., Li, M., and Chance, R. (2020). Trace metal fractional solubility in size-segregated aerosols from the tropical eastern Atlantic Ocean. *Glob. Biogeochem. Cycles*, **34**(6), e2019GB006510.

Bauer S. E., Balkanski Y., Schulz M. and Hauglustaine D. A. (2004) Global modeling of heterogeneous

chemistry on mineral aerosol surfaces: Influence on tropospheric ozone chemistry and comparison to observations. *J. Geophys. Res.* **109**, 1–17.

Bigalke M., Weyer S., Kobza J. and Wilcke W. (2010) Stable Cu and Zn isotope ratios as tracers of sources and transport of Cu and Zn in contaminated soil. *Geochim. Cosmochim. Acta* **74**, 6801–6813.

Borrok D. M., Gieré R., Ren M. and Landa E. R. (2010) Zinc isotopic composition of particulate matter generated during the combustion of coal and coal + tire-derived fuels. *Environ. Sci. Technol.* **44**, 9219–9224.

Boyce D. G., Lewis M. R. and Worm B. (2010) Global phytoplankton decline over the past century. *Nature* **466**, 591–596.

Brand L. E., Sunda W. G. and Guillard R. R. L. (1986) Reduction of marine phytoplankton reproduction rates by copper and cadmium. *J. Exp. Mar. Bio. Ecol.* **96**, 225–250.

Bridgestock L., Van De Flierdt T., Rehkämper M., Paul M., Middag R., Milne A., Lohan M. C., Baker A. R., Chance R., Khondoker R., Strekopytov S., Humphreys-Williams E., Achterberg E. P., Rijkenberg M. J. A., Gerringa L. J. A. and De Baar H. J. W. (2016) Return of naturally sourced Pb to Atlantic surface waters. *Nat. Commun.* **7**.

Bridgestock L. J. (2015) Tracing the cycling of Pb and Cd from natural and anthropogenic sources through the troposphere and ocean. Ph. D. thesis. Imperial College London.

Bridgestock L. J., Williams H., Rehkämper M., Larner F., Giscard M. D., Hammond S., Coles B., Andreasen R., Wood B. J., Theis K. J., Smith C. L., Benedix G. K. and Schönbächler M. (2014) Unlocking the zinc isotope systematics of iron meteorites. *Earth Planet. Sci. Lett.* **400**, 153–164.

Bridgestock L., Rehkämper M., van de Flierdt T., Murphy K., Khondoker R., Baker A. R., Chance R., Strekopytov S., Humphreys-Williams E. and Achterberg E. P. (2017) The Cd isotope composition of atmospheric aerosols from the Tropical Atlantic Ocean. *Geophys. Res. Lett.* **44**, 2932–2940.

Bruland K. W., Middag R. and Lohan M. C. (2013) Controls of Trace Metals in Seawater. In *Treatise on Geochemistry: Second Edition* Elsevier Ltd. pp. 19–51.

Bruland K. W., Rue E. L. and Smith G. J. (2001) Iron and macronutrients in California coastal upwelling regimes: Implications for diatom blooms. *Limnol. Oceanogr.* **46**, 1661–1674.

Buck, K.N., Moffett, J., Barbeau, K.A., Bundy, R.M., Kondo, Y. and Wu, J.F., (2012) The organic complexation of iron and copper: an intercomparison of competitive ligand exchange-adsorptive cathodic stripping voltammetry (CLE-ACSV) techniques. *Limnol Oceanogr-Meth* **10**, 496-515

Campos, M.L.A.M. and van den Berg, C.M.G. (1994) Determination of copper complexation in sea water by cathodic stripping voltammetry and ligand competition with salicylaldoxime. *Anal. Chim. Acta* **284**, 481-496.

Chen J., Gaillardet J. and Louvat P. (2008) Zinc isotopes in the Seine River waters, France: A probe of anthropogenic contamination. *Environ. Sci. Technol.* **42**, 6494–6501.

Chester R. (1993) Defining the chemical character of aerosols from the atmosphere of the Mediterranean Sea and surrounding regions. *Oceanol. Acta* **16**, 231–246.

Chester R. and Jickells T. (2012) *Marine Geochemistry*. 3rd ed., John Wiley & Sons, Incorporated.

Church T. M., Véron A., Patterson C. C., Settle D., Erel Y., Maring H. R. and Flegal A. R. (1990) Trace elements in the North Atlantic troposphere: shipboard results of precipitation and aerosols. *Global Biogeochem. Cycles* **4**, 431–443.

Cloquet C., Carignan J. and Libourel G. (2006a) Isotopic composition of Zn and Pb atmospheric depositions in an urban/periurban area of northeastern France. *Environ. Sci. Technol.* **40**, 6594–6600.

Cloquet C., Carignan J., Libourel G., Sterckeman T. and Perdrix E. (2006b) Tracing source pollution in soils using cadmium and lead isotopes. *Environ. Sci. Technol.* **40**, 2525–2530.

Coale K. H. and Bruland K. W. (1988) Copper complexation in the Northeast Pacific. *Limnol. Oceanogr.* **33**, 1084–1101.

Conway T. M. and John S. G. (2014) The biogeochemical cycling of zinc and zinc isotopes in the North Atlantic Ocean. *Global Biogeochem. Cycles* **28**, 1111–1128.

Conway T. M. and John S. G. (2015) The cycling of iron, zinc and cadmium in the North East Pacific Ocean - Insights from stable isotopes. *Geochim. Cosmochim. Acta* **164**, 262–283.

Desboeufs K. V., Sofikitis A., Losno R., Colin J. L. and Ausset P. (2005) Dissolution and solubility of trace metals from natural and anthropogenic aerosol particulate matter. *Chemosphere* **58**, 195–203.

Dong S., Ochoa Gonzalez R., Harrison R. M., Green D., North R., Fowler G. and Weiss D. (2017) Isotopic signatures suggest important contributions from recycled gasoline, road dust and non-exhaust traffic sources for copper, zinc and lead in PM10 in London, United Kingdom. *Atmos. Environ.* **165**, 88–98.

Dong S., Weiss D. J., Strekopytov S., Kreissig K., Sun Y., Baker A. R. and Formenti P. (2013) Stable isotope ratio measurements of Cu and Zn in mineral dust (bulk and size fractions) from the Taklimakan Desert and the Sahel and in aerosols from the eastern tropical North Atlantic Ocean. *Talanta* **114**, 103–109.

Duce R. A., Liss P. S., Merrill J. T., Atlas E. L., Buat-Menard P., Hicks B. B., Miller J. M., Prospero J. M., Arimoto R., Church T. M., Ellis W., Galloway J. N., Hansen L., Jickells T. D., Knap A. H., Reinhardt K. H., Schneider B., Soudine A., Tokos J. J., Tsunogai S., Wollast R. and Zhou M. (1991) The atmospheric input of trace species to the world ocean. *Global Biogeochem. Cycles* **5**, 193–259.

Ellwood, M.J. and van den Berg, C.M.G. (2000) Zinc speciation in the northeast Atlantic Ocean. *Mar. Chem*. **68**, 295-306.

Gao Y., Nelson E. D., Field M. P., Ding Q., Li H., Sherrell R. M., Gigliotti C. L., Van Ry D. A., Glenn T. R. and Eisenreich S. J. (2002) Characterization of atmospheric trace elements on PM2.5 particulate matter over the New York-New Jersey harbor estuary. *Atmos. Environ.* **36**, 1077–1086.

Gelly R., Fekiacova Z., Guihou A., Doelsch E., Deschamps P. and Keller C. (2019) Lead, zinc, and copper redistributions in soils along a deposition gradient from emissions of a Pb-Ag smelter decommissioned 100 years ago. *Sci. Total Environ.* **665**, 502–512.

Goudie A. S. and Middleton N. J. (2001) Saharan dust storms: nature and consequences. *Earth-Science Rev.* **56**, 179–204.

Gustavson K. and Wängberg S. Å. (1995) Tolerance induction and succession in microalgae communities exposed to copper and atrazine. *Aquat. Toxicol.* **32**, 283–302.

Heinold B., Tegen I., Bauer S. and Wendisch M. (2011) Regional modelling of Saharan dust biomass-burning smoke: Part 2: Direct radiative forcing atmospheric dynamic response. *Tellus* **63B**, 800–813.

Helmers E. and Schrems O. (1995) Wet deposition of metals to the tropical North and the South Atlantic ocean. *Atmos. Environ.* **29**, 2475–2484.

Hong S., Candelone J. P., Patterson C. C. and Boutron C. F. (1996) History of ancient copper smelting pollution during Roman and medieval times recorded in Greenland ice. *Science.* **272**, 246–249.

Hulskotte J. H. J., Schaap M. and Visschedijk A. J. H. (2007) Brake wear from vehicles as an important source of diffuse copper pollution. *Water Sci. Technol.* **56**, 223–231.

Jickells T.D. (1995) Atmospheric inputs of metals and nutrients to the oceans: their magnitude and effects. *Mar. Chem.* **48**, 199–214.

Jickells, T.D., Baker, A.R. and Chance, R. (2016) Atmospheric transport of trace elements and nutrients to the oceans. *Philos. Trans. Royal Soc. A* **374**, 20150286.

Johansson L., Jalkanen J. P. and Kukkonen J. (2017) Global assessment of shipping emissions in 2015 on a high spatial and temporal resolution. *Atmos. Environ.* **167**, 403–415.

John S. G. and Conway T. M. (2014) A role for scavenging in the marine biogeochemical cycling of zinc and zinc isotopes. *Earth Planet. Sci. Lett.* **394**, 159–167.

John S. G., Genevieve Park J., Zhang Z. and Boyle E. A. (2007) The isotopic composition of some common

forms of anthropogenic zinc. *Chem. Geol.* **245**, 61–69.

Jordi A., Basterretxea G., Tovar-Sanchez A., Alastuey A. and Querol X. (2012) Copper aerosols inhibit phytoplankton growth in the Mediterranean Sea. *Proc. Natl. Acad. Sci.* **109**, 21246–21249.

Labonne M., Bréon F. M. and Chevallier F. (2007) Injection height of biomass burning aerosols as seen from a spaceborne lidar. *Geophys. Res. Lett.* **34**.

Lantzy R. J. and Mackenzie F. T. (1979) Atmospheric trace metals: global cycles and assessment of man's impact. *Geochim. Cosmochim. Acta* **43**, 511–525.

Larner F., Rehkämper M., Coles B. J., Kreissig K., Weiss D. J., Sampson B., Unsworth C. and Strekopytov S. (2011) A new separation procedure for Cu prior to stable isotope analysis by MC-ICP-MS. *J. Anal. At. Spectrom.* **26**, 1627–1632.

Laurent B., Marticorena B., Bergametti G., Léon J. F. and Mahowald N. M. (2008) Modeling mineral dust emissions from the Sahara desert using new surface properties and soil database. *J. Geophys. Res. Atmos.* **113**, 1–20.

Lemaitre N., de Souza G. F., Archer C., Wang R. M., Planquette H., Sarthou G. and Vance D. (2020) Pervasive sources of isotopically light zinc in the North Atlantic Ocean. *Earth Planet. Sci. Lett.* **539**, 116216.

Levy J. L., Stauber J. L. and Jolley D. F. (2007) Sensitivity of marine microalgae to copper: The effect of biotic factors on copper adsorption and toxicity. *Sci. Total Environ.* **387**, 141–154.

Liao W. H., Takano S., Tian H. A., Chen H. Y., Sohrin Y. and Ho T. Y. (2021) Zn elemental and isotopic features in sinking particles of the South China Sea: Implications for its sources and sinks. *Geochim. Cosmochim. Acta* **314**, 68–84.

Liao W. H., Takano S., Yang S. C., Huang K. F., Sohrin Y. and Ho T. Y. (2020) Zn Isotope Composition in the Water Column of the Northwestern Pacific Ocean: The Importance of External Sources. *Global Biogeochem. Cycles* **34**, 1–18.

Little S. H., Archer C., Milne A., Schlosser C., Achterberg E. P., Lohan M. C. and Vance D. (2018) Paired dissolved and particulate phase Cu isotope distributions in the South Atlantic. *Chem. Geol.* **502**, 29–43.

Little S. H., Munson S., Prytulak J., Coles B. J., Hammond S. J. and Widdowson M. (2019) Cu and Zn isotope fractionation during extreme chemical weathering. *Geochim. Cosmochim. Acta* **263**, 85–107.

Little S. H., Vance D., Walker-Brown C. and Landing W. M. (2014) The oceanic mass balance of copper and zinc isotopes, investigated by analysis of their inputs, and outputs to ferromanganese oxide sediments. *Geochim. Cosmochim. Acta* **125**, 673–693.

Lopez J. S., Lee L. and Mackey K. R. M. (2019) The Toxicity of Copper to Crocosphaera watsonii and Other Marine Phytoplankton: A Systematic Review. *Front. Mar. Sci.* **5**, 1–13.

Maenhaut W., Salma I., Cafmeyer J., Annegarn H. J. and Andreae M. O. (1996) Regional atmospheric aerosol composition and sources in the eastern Transvaal, South Africa, and impact of biomass burning. *J. Geophys. Res. Atmos.* **101**, 23631–23650.

Mahowald N. M., Hamilton D. S., Mackey K. R. M., Moore J. K., Baker A. R., Scanza R. A. and Zhang Y. (2018) Aerosol trace metal leaching and impacts on marine microorganisms. *Nat. Commun.* **9**, 1–15.

Maréchal C. N., Télouk P. and Albarède F. (1999) Precise analysis of copper and zinc isotopic compositions by plasma-source mass spectrometry. *Chem. Geol.* **156**, 251–273.

Mathur R., Titley S., Barra F., Brantley S., Wilson M., Phillips A., Munizaga F., Maksaev V., Vervoort J. and Hart G. (2009) Exploration potential of Cu isotope fractionation in porphyry copper deposits. *J. Geochemical Explor.* **102**, 1–6.

Mattielli N., Petit J. C. J., Deboudt K., Flament P., Perdrix E., Taillez A., Rimetz-Planchon J. and Weis D. (2009) Zn isotope study of atmospheric emissions and dry depositions within a 5 km radius of a Pb-

Zn refinery. *Atmos. Environ.* **43**, 1265–1272.

Meskhidze, N., Völker, C., Al-Abadleh, H.A., Barbeau, K., Bressac, M., Buck, C., Bundy, R.M., Croot, P., Feng, Y., Ito, A., Johansen, A.M., Landing, W.M., Mao, J., Myriokefalitakis, S., Ohnemus, D., Pasquier, B. and Ye, Y. (2019) Perspective on identifying and characterizing the processes controlling iron speciation and residence time at the atmosphere-ocean interface. *Mar. Chem.* **217**, 103704.

Mihaljevič M., Jarošíková A., Ettler V., Vaněk A., Penížek V., Kříbek B., Chrastný V., Sracek O., Trubač J., Svoboda M. and Nyambe I. (2018) Copper isotopic record in soils and tree rings near a copper smelter, Copperbelt, Zambia. *Sci. Total Environ.* **621**, 9–17.

Millero F. J., Feistel R., Wright D. G. and McDougall T. J. (2008) The composition of Standard Seawater and the definition of the Reference-Composition Salinity Scale. *Deep. Res. Part I Oceanogr. Res. Pap.* **55**, 50–72.

Moffett J. W. and Brand L. E. (1996) Production of strong, extracellular Cu chelators by marine cyanobacteria in response to Cu stress. *Limnol. Oceanogr.* **41**, 388–395.

Moffett J. W., Brand L. E., Croot P. L. and Barbeau K. A. (1997) Cu speciation and cyanobacterial distribution in harbors subject to anthropogenic Cu inputs. *Limnol. Oceanogr.* **42**, 789–799.

Moffett J. W. and Dupont C. (2007) Cu complexation by organic ligands in the sub-arctic NW Pacific and Bering Sea. *Deep. Res. Part I Oceanogr. Res. Pap.* **54**, 586–595.

Moore C. M., Mills M. M., Arrigo K. R., Berman-Frank I., Bopp L., Boyd P. W., Galbraith E. D., Geider R. J., Guieu C., Jaccard S. L., Jickells T. D., La Roche J., Lenton T. M., Mahowald N. M., Marañón E., Marinov I., Moore J. K., Nakatsuka T., Oschlies A., Saito M. A., Thingstad T. F., Tsuda A. and Ulloa O. (2013) Processes and patterns of oceanic nutrient limitation. *Nat. Geosci.* **6**, 701–710.

Moynier F., Vance D., Fujii T. and Savage P. (2017) The Isotope Geochemistry of Zinc and Copper. *Rev. Mineral. Geochemistry* **82**, 543–600.

Nielsen S. G., Rehkämper M., Baker J. and Halliday A. N. (2004) The precise and accurate determination of thallium isotope compositions and concentrations for water samples by MC-ICPMS. *Chem. Geol.* **204**, 109–124.

Novak M., Sipkova A., Chrastny V., Stepanova M., Voldrichova P., Veselovsky F., Prechova E., Blaha V., Curik J., Farkas J., Erbanova L., Bohdalkova L., Pasava J., Mikova J., Komarek A. and Krachler M. (2016) Cu-Zn isotope constraints on the provenance of air pollution in Central Europe: Using soluble and insoluble particles in snow and rime. *Environ. Pollut.* **218**, 1135–1146.

Nriagu J. O. (1979) Global inventory of natural and anthropogenic emissions of trace metals to the atmosphere. *Nature* **279**, 409–411.

Nriagu J. O. and Pacyna J. M. (1988) Quantitative assessment of worldwide contamination of air, water and soils by trace metals. *Nature* **332**, 134–139.

Ochoa Gonzalez R., Strekopytov S., Amato F., Querol X., Reche C. and Weiss D. (2016) New Insights from Zinc and Copper Isotopic Compositions into the Sources of Atmospheric Particulate Matter from Two Major European Cities. *Environ. Sci. Technol.* **50**, 9816–9824.

Ochoa Gonzalez R. and Weiss D. (2015) Zinc Isotope Variability in Three Coal-Fired Power Plants: A Predictive Model for Determining Isotopic Fractionation during Combustion. *Environ. Sci. Technol.* **49**, 12560–12567.

Pacyna J. M. and Pacyna E. G. (2001) An assessment of global and regional emissions of trace metals to the atmosphere from anthropogenic sources worldwide. *Environ. Rev.* **9**, 269–298.

Patterson C. C. and Settle D. M. (1987) Review of data on eolian fluxes of industrial and natural lead to the lands and seas in remote regions on a global scale. *Mar. Chem.* **22**, 137–162.

Paytan A., Mackey K. R. M., Chen Y., Lima I. D., Doney S. C., Mahowald N., Labiosa R. and Post A. F. (2009) Toxicity of atmospheric aerosols on marine phytoplankton. *Proc. Natl. Acad. Sci. U. S. A.* **106**, 4601–4605.

Powell C. F., Baker A. R., Jickells T. D., W. Bange H., Chance R. J. and Yodle C. (2015) Estimation of the atmospheric flux of nutrients and trace metals to the eastern tropical North Atlantic Ocean. *J. Atmos. Sci.* **72**, 4029–4045.

Quigg A., Reinfelder J. R. and Fisher N. S. (2006) Copper uptake kinetics in diverse marine phytoplankton. *Limnol. Oceanogr.* **51**, 893–899.

Reuer M. K. and Weiss D. J. (2002) Anthropogenic lead dynamics in the terrestrial and marine environment. *Philos. Trans. R. Soc. A Math. Phys. Eng. Sci.* **360**, 2889–2904.

Roshan S., DeVries T., Wu J. and Chen G. (2018) The Internal Cycling of Zinc in the Ocean. *Global Biogeochem. Cycles* **32**, 1833–1849.

Rudnick R. L. and Gao S. (2003) Composition of the Continental Crust. In *Treatise on Geochemistry: Second Edition* Elsevier Ltd. pp. 1–64.

Samanta M., Ellwood M. J., Sinoir M. and Hassler C. S. (2017) Dissolved zinc isotope cycling in the Tasman Sea, SW Pacific Ocean. *Mar. Chem.* **192**, 1–12.

Sarthou G., Baker A. R., Blain S., Achterberg E. P., Boye M., Bowie A. R., Croot P., Laan P., De Baar H. J. W., Jickells T. D. and Worsfold P. J. (2003) Atmospheric iron deposition and sea-surface dissolved iron concentrations in the eastern Atlantic Ocean. *Deep. Res. Part I Oceanogr. Res. Pap.* **50**, 1339–1352.

Schleicher N. J., Dong S., Packman H., Little S. H., Ochoa Gonzalez R., Najorka J., Sun Y. and Weiss D. J. (2020) A Global Assessment of Copper, Zinc, and Lead Isotopes in Mineral Dust Sources and Aerosols. *Front. Earth Sci.* **8**, 1–20.

Schlosser C., Klar J. K., Wake B. D., Snow J. T., Honey D. J., Woodward E. M. S., Lohan M. C., Achterberg E. P. and Mark Moore C. (2014) Seasonal ITCZ migration dynamically controls the location of the (sub)tropical Atlantic biogeochemical divide. *Proc. Natl. Acad. Sci. U. S. A.* **111**, 1438–1442.

Semeniuk D. M., Bundy R. M., Payne C. D., Barbeau K. A. and Maldonado M. T. (2015) Acquisition of organically complexed copper by marine phytoplankton and bacteria in the northeast subarctic Pacific Ocean. *Mar. Chem.* **173**, 222–233.

Shelley R. U., Landing W. M., Ussher S. J., Planquette H. and Sarthou G. (2018) Regional trends in the fractional solubility of Fe and other metals from North Atlantic aerosols (GEOTRACES cruises GA01 and GA03) following a two-stage leach. *Biogeosciences* **15**, 2271–2288.

Shiel A. E., Weis D. and Orians K. J. (2010) Evaluation of zinc, cadmium and lead isotope fractionation during smelting and refining. *Sci. Total Environ.* **408**, 2357–2368.

Sholkovitz E. R., Sedwick P. N. and Church T. M. (2010) On the fractional solubility of copper in marine aerosols: Toxicity of aeolian copper revisited. *Geophys. Res. Lett.* **37**, 1–4.

Sieber M., Conway T. M., de Souza G. F., Hassler C. S., Ellwood M. J. and Vance D. (2020) Cycling of zinc and its isotopes across multiple zones of the Southern Ocean: Insights from the Antarctic Circumnavigation Expedition. *Geochim. Cosmochim. Acta* **268**, 310–324.

Siebert C., Nägler T. F. and Kramers J. D. (2001) Determination of molybdenum isotope fractionation by double-spike multicollector inductively coupled plasma mass spectrometry. *Geochemistry, Geophys. Geosystems* **2**, 1032.

Sivry Y., Riotte J., Sonke J. E., Audry S., Schäfer J., Viers J., Blanc G., Freydier R. and Dupré B. (2008) Zn isotopes as tracers of anthropogenic pollution from Zn-ore smelters The Riou Mort-Lot River system. *Chem. Geol.* **255**, 295–304.

Souto-Oliveira C. E., Babinski M., Araújo D. F. and Andrade M. F. (2018) Multi-isotopic fingerprints (Pb, Zn, Cu) applied for urban aerosol source apportionment and discrimination. *Sci. Total Environ.* **626**, 1350–1366.

Souto-Oliveira C. E., Babinski M., Araújo D. F., Weiss D. J. and Ruiz I. R. (2019) Multi-isotope approach of Pb, Cu and Zn in urban aerosols and anthropogenic sources improves tracing of the atmospheric pollutant sources in megacities. *Atmos. Environ.* **198**, 427–437.

Sunda W. (1976) The relationship between cupric ion activity and the toxicity of copper to phytoplankton. Ph. D. thesis. Massachusetts Institute of Technology.

Sunda W. G. (1989) Trace metal interactions with marine phytoplankton. *Biol. Oceanogr.* **6**, 411–442.

Sunda W. G. and Huntsman S. A. (1995) Cobalt and zinc interreplacement in marine phytoplankton : Biological and geochemical implications. *Limnol. Oceanogr.* **40**, 1404–1417.

Takano S., Tanimizu M., Hirata T. and Sohrin Y. (2014) Isotopic constraints on biogeochemical cycling of copper in the ocean. *Nat. Commun.* **5**, 1–7.

Thapalia A., Borrok D. M., Van Metre P. C., Musgrove M. and Landa E. R. (2010) Zn and Cu isotopes as tracers of anthropogenic contamination in a sediment core from an Urban Lake. *Environ. Sci. Technol.* **44**, 1544–1550.

Thompson C. M., Ellwood M. J. and Wille M. (2013) A solvent extraction technique for the isotopic measurement of dissolved copper in seawater. *Anal. Chim. Acta* **775**, 106–113.

Thuróczy C. E., Boye M. and Losno R. (2010) Dissolution of cobalt and zinc from natural and anthropogenic dusts in seawater. *Biogeosciences* **7**, 1927–1936.

Tositti L., Brattich E., Masiol M. and Baldacci D. (2014) Source apportionment of particulate matter in a large city of southeastern Po Valley (Bologna , Italy). *Environ. Sci. Pollut. Res. Vol.* **21**, 872–890.

Tsyro S., Aas W., Soares J., Sofiev M., Berge H. and Spindler G. (2011) Modelling of sea salt concentrations over Europe: Key uncertainties and comparison with observations. *Atmos. Chem. Phys.* **11**, 10367–10388.

Turner D. R., Hassellöv I.-M., Ytreberg E. and Rutgersson A. (2017) Shipping and the environment: Smokestack emissions, scrubbers and unregulated oceanic consequences. *Elem. Sci. Anthr.* **5**, 1–10.

Vallee B. L. and Auld D. S. (1990) Zinc Coordination, Function, and Structure of Zinc Enzymes and Other Proteins. *Biochemistry* **29**, 5647–5659.

Vance D., de Souza G. F., Zhao Y., Cullen J. T. and Lohan M. C. (2019) The relationship between zinc, its isotopes, and the major nutrients in the North-East Pacific. *Earth Planet. Sci. Lett.* **525**, 115748.

Vanderstraeten A., Bonneville S., Gili S., de Jong J., Debouge W., Claeys P. and Mattielli N. (2020) First Multi-Isotopic (Pb-Nd-Sr-Zn-Cu-Fe) Characterisation of Dust Reference Materials (ATD and BCR-723): A Multi-Column Chromatographic Method Optimised to Trace Mineral and Anthropogenic Dust Sources. *Geostand. Geoanalytical Res.* **44**, 307–329.

Wan Z., Zhu M., Chen S. and Sperling D. (2016) Pollution: Three steps to a green shipping industry. *Nature* **530**, 275–277.

Wang F. J., Chen Y., Guo Z. G., Gao H. W., Mackey K. R., Yao X. H., Zhuang G. S. and Paytan A. (2017) Combined effects of iron and copper from atmospheric dry deposition on ocean productivity. *Geophys. Res. Lett.* **44**, 2546–2555.

Wang R. M., Archer C., Bowie A. R. and Vance D. (2019) Zinc and nickel isotopes in seawater from the Indian Sector of the Southern Ocean: The impact of natural iron fertilization versus Southern Ocean hydrography and biogeochemistry. *Chem. Geol.* **511**, 452–464.

Weber T., John S., Tagliabue A. and DeVries T. (2018) Biological uptake and reversible scavenging of zinc in the global ocean. *Science.* **361**, 72–76.

Van Der Werf G. R., Randerson J. T., Giglio L., Collatz G. J., Mu M., Kasibhatla P. S., Morton D. C., Defries R. S., Jin Y. and Van Leeuwen T. T. (2010) Global fire emissions and the contribution of deforestation, savanna, forest, agricultural, and peat fires (1997-2009). *Atmos. Chem. Phys.* **10**, 11707–11735.

White W. H. (2008) Chemical markers for sea salt in IMPROVE aerosol data. *Atmos. Environ.* **42**, 261–274.

Yin N. H., Sivry Y., Benedetti M. F., Lens P. N. L. and van Hullebusch E. D. (2016) Application of Zn isotopes in environmental impact assessment of Zn-Pb metallurgical industries: A mini review. *Appl. Geochemistry* **64**, 128–135.

Zhang X., Huang J., Gong Y., Zhang L. and Huang F. (2022) Climate influence on zinc isotope variations in a loess–paleosol sequence of the Chinese Loess Plateau. *Geochim. Cosmochim. Acta* **321**, 115–132.

Zhao Y., Vance D., Abouchami W. and de Baar H. J. W. (2014) Biogeochemical cycling of zinc and its isotopes in the Southern Ocean. *Geochim. Cosmochim. Acta* **125**, 653–672.

Zoller W. H., Gladney E. S. and Duce R. A. (1974) Atmospheric Concentrations and Sources of Trace Metals at the South Pole. *Science.* **183**, 198–200.

Declaration of interests

☐The authors declare that they have no known competing financial interests or personal relationships that could have appeared to influence the work reported in this paper.

☒The authors declare the following financial interests/personal relationships which may be considered as potential competing interests:
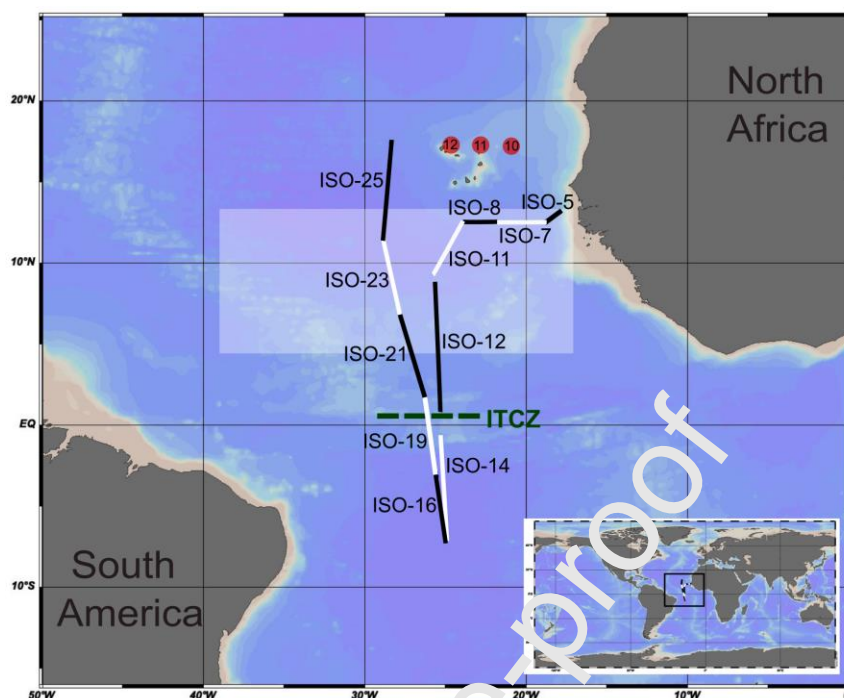
Figure 1: Map of aerosol sampling locations from the GEOTRACES GA06 section cruise (D361, February–March 2011). The white and black marks indicate the distance the aerosols were collected over. The semi-transparent white square represents the approximate region of the North African dust plume at the time of collection (Bridgestock et al., 2016) and the dashed line represents the approximate location of the ITCZ (Schlosser et al., 2014). The red circles labelled 10, 11 and 12 are station locations from the GEOTRACES GA03 cruise (Conway and John, 2014). Schlitzer, R., Ocean Data View, http://odv.awi.de, 2016.

Table 1: Filter blank results, including Zn and Cu masses per filter, and δ^{66}Zn values

	Zn mass (ng)	δ^{66}Zn (‰)	Cu mass (ng)
Cassette blank total digest	565	0.04	37
Filter blank total digest(s)	459	0.16	59, 122
Exposure blank total digest(s)	*2219, 3767*	0.28, nd	44
Mean:	**512**	**0.10**	**66**
Cassette blank leachate	*2123*	*0.14*	40
Filter blank leachate(s)	**574**	**0.02**	15, 26
Exposure blank leachate(s)	161, 232	0.04, 0.08	25
Mean:	322	0.05	**27**

Values in italics are considered overestimates: see discussion in the main text and the Supplementary Text. Values in bold are those used in blank subtraction of sample concentrations (Table 2, see also Table S3). nd = not measured.

Table 2: Zn and Cu concentrations and isotope compositions of aerosols collected during the GEOTRACES GA06 cruise. OC in the AMBT group (air mass back trajectory group) refers to oceanic samples, which spent the previous five days over the ocean, and NA refers to samples originating from North Africa

Sample	AMBT group	Zn				Cu			
		[Zn] (ng m^{-3})	uncert^a	$\delta^{66}Zn_{JMC-Lyon}$ (‰)	2 SD	[Cu] (ng m^{-3})	uncert^a	$\delta^{65}Cu_{NIST976}$ (‰)	2 SD
ISO-05-2 (Total Digest)	NA	7.69	0.25	0.15	0.08	2.75	0.03	-0.15	0.08
ISO-07 (Total Digest)	NA	5.37	0.33	0.17	0.08	2.52	0.04	0.15	0.08
ISO-08 (Total Digest)	NA	4.02	0.26	0.41	0.08	1.44	0.04	0.08	0.08
ISO-11 (Total Digest)	NA	1.67	0.39	0.09	0.08	0.47	0.06	-0.34	0.08
ISO-12 (Total Digest)	NA	10.07	0.37	0.23	0.08	4.23	0.05	0.15	0.08
ISO-14 (Total Digest)	OC	2.70	0.16	0.15	0.08	1.09	0.02	0.26	0.08
ISO-16 (Total Digest)	OC	1.05	0.16	0.11	0.08	0.41	0.02		
ISO-19 (Total Digest)	OC	4.19	0.22	0.26	0.08	2.14	0.03		
ISO-21 (Total Digest)	NA	5.02	0.17	0.24	0.08	2.05	0.02	0.15	0.08
ISO-23 (Total Digest)	NA	3.03	0.17	-0.02	0.08	1.00	0.02	0.26	0.08
ISO-25 (Total Digest)	NA	0.78	0.11	0.12	0.08	0.20	0.02	0.03	0.08
ISO-05 (Leachate)	NA	1.26	0.24	0.25	0.08	0.41	0.01		
ISO-07 (Leachate)	NA	2.29	0.34			0.29	0.02		
ISO-08 (Leachate)	NA	0.29	0.15	0.17	0.08	0.11	0.01		
ISO-11 (Leachate)	NA	1.97	0.44	0.00	0.08	0.12	0.02	0.03	0.08
ISO-12 (Leachate)	NA	4.50	0.40	0.14	0.08	1.81	0.02		
ISO-14 (Leachate)	OC	1.82	0.11	0.17	0.08	0.84	0.01	0.27	0.08
ISO-16 (Leachate)	OC	1.42	0.19			0.29	0.01		
ISO-19 (Leachate)	OC	2.68	0.24			1.40	0.01		
ISO-21 (Leachate)	NA	2.62	0.19	0.21	0.08	0.68	0.01		
ISO-23 (Leachate)	NA	2.44	0.19			0.79	0.01		
ISO-25 (Leachate)	NA	1.05	0.13	0.14	0.08	0.23	0.01		

^{a}uncertainties for [Zn] and [Cu] were calculated by standard error propagation methods using the filter blank and the total sample filter mass multiplied by the resultant concentration.

2 SD is the long-term external reproducibility on the relevant secondary standard.
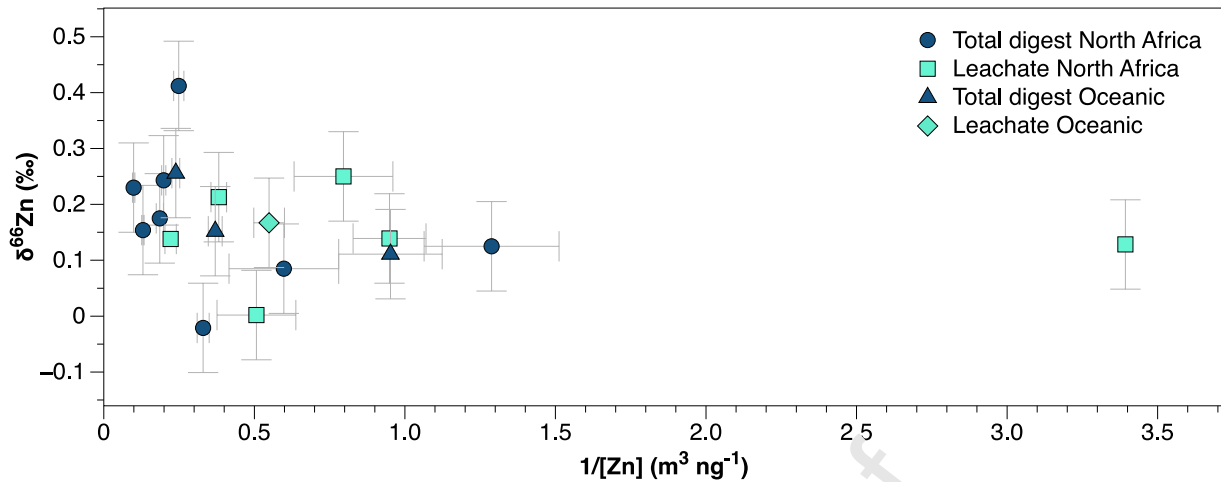
Figure 2: Zn isotope compositions ($\delta^{66}Zn_{JMC}$) plotted versus the inverse of atmospheric Zn concentrations (1/[Zn]). For clarity, the large uncertainty (±3.3 m^3 ng^{-1}) associated with the data point with the highest 1/[Zn] value of 3.4 m^3 ng^{-1} is not shown.
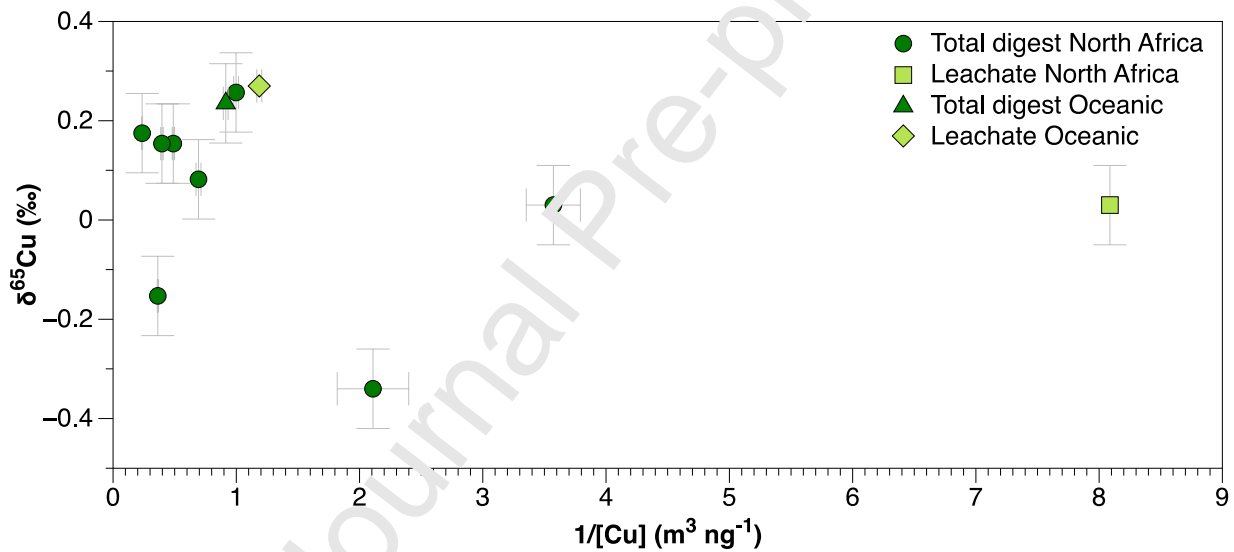
Figure 3: Cu isotope compositions ($\delta^{65}Cu_{NIST}$) plotted versus the inverse of atmospheric Cu concentrations (1/[Cu]). For clarity, the large uncertainty (±3.1 m^3 ng^{-1}) associated with the data point with the highest 1/[Cu] value of 8.1 m^3 ng^{-1} is not shown.

Table 3: Zn and Cu isotope compositions, concentration and fractional solubilities of Arizona Test Dust (ATD)

	$\delta^{66}Zn_{JMC-Lyon}$ (‰)	2 SD	[Zn] (ppm)	Zn Fractional Solubility (%)	$\delta^{65}Cu_{NIST}$ (‰)	2 SD	[Cu] (ppm)	Cu Fractional Solubility (%)
ATD 1 Total digest	0.33	0.08	111.6	13.5	0.21	0.08	37.6	7.0
ATD 2 Total digest	0.27	0.08			0.20	0.08		
ATD 3 Total digest	0.27	0.08	114.0	15.6	0.18	0.08	39.8	8.1
ATD 4 Leachate	0.47	0.08	15.1		0.61	0.08	2.6	
ATD 5 Leachate	0.52	0.08	17.4		0.57	0.08	3.2	
ATD 6 Leachate	0.52	0.08	17.7		0.64	0.08	3.2	

2 SD is the long-term external reproducibility on the relevant secondary standard

Table 4: Zn and Cu enrichment factors and fractional solubilities plus Al concentrations

Sample	AMBT group	[Al] (ng m^{-3})	Zn				Cu			
			EF	uncert[a]	Fractional Solubility (%)	uncert[b]	EF	uncert[a]	Fractional Solubility (%)	uncert[b]
ISO-05-2 (Total Digest)	NA	5808	1.8	0.4	16	3	1.2	0.2	15	1
ISO-07 (Total Digest)	NA	1935	1.3	0.2	43	5	1.1	0.1	12	1
ISO-08 (Total Digest)	NA	3482	3.4	0.2	7	4	3.8	0.1	7	1
ISO-11 (Total Digest)	NA	1148	3.1	0.1	118	38	3.2	0.0	26	6
ISO-12 (Total Digest)	NA	3891	1.4	0.1	45	4	1.2	0.0	43	1
ISO-14 (Total Digest)	OC	137	23.9	1.5	67	8	23.3	0.5	77	2
ISO-16 (Total Digest)	OC	68	18.7	2.9	136	27	17.9	1.1	70	5
ISO-19 (Total Digest)	OC	728	7.0	0.4	64	7	8.6	0.1	66	1
ISO-21 (Total Digest)	NA	1527	4.0	0.1	52	4	3.9	0.0	33	1
ISO-23 (Total Digest)	NA	667	5.5	0.3	81	8	4.4	0.1	79	2
ISO-25 (Total Digest)	NA	74	12.5	1.9	136	26	11.2	0.7	84	5

[a] uncertainties for EF were calculated by error propagation using filter blank values and the uncorrected filter masses for Zn, Cu and Al

[b] uncertainties for fractional solubilities were estimated by propagating the total digest and leachate aerosol concentrations and their associated errors
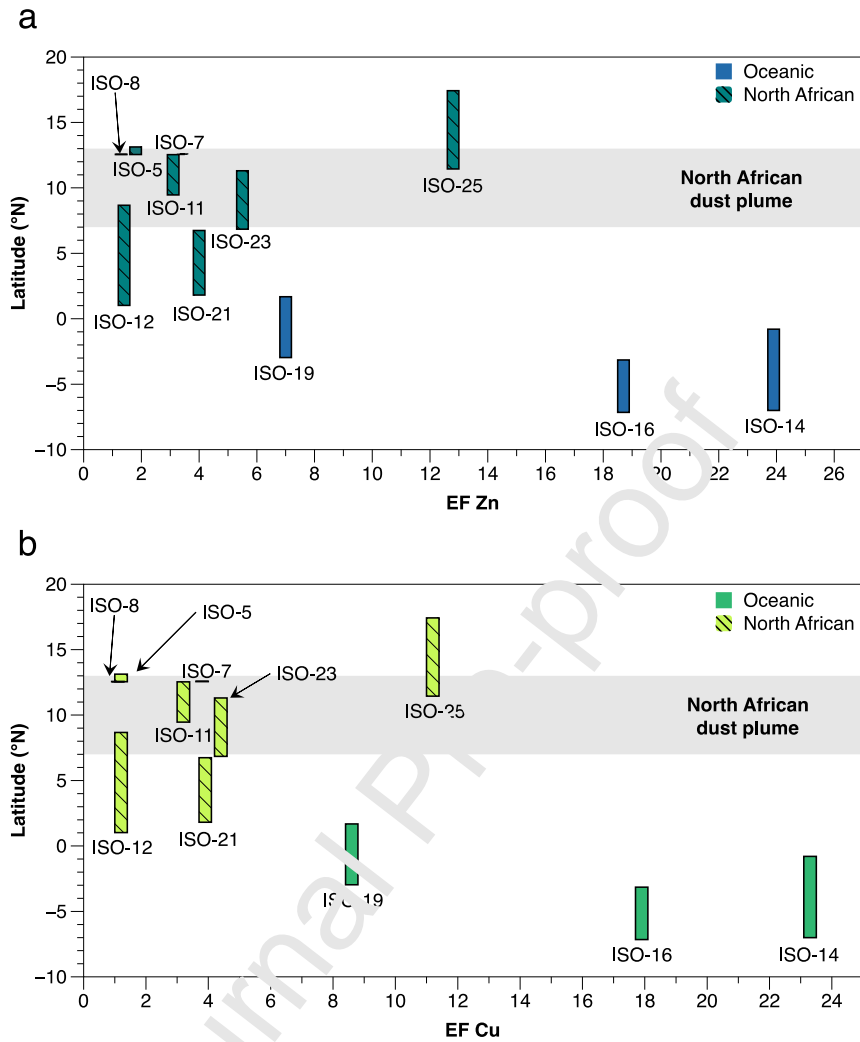
Figure 4: a) Zn enrichment factors plotted against latitude b) Cu enrichment factors plotted against latitude. Both include a grey band indicating the latitudinal position of the North African dust plume (Bridgestock et al., 2016)
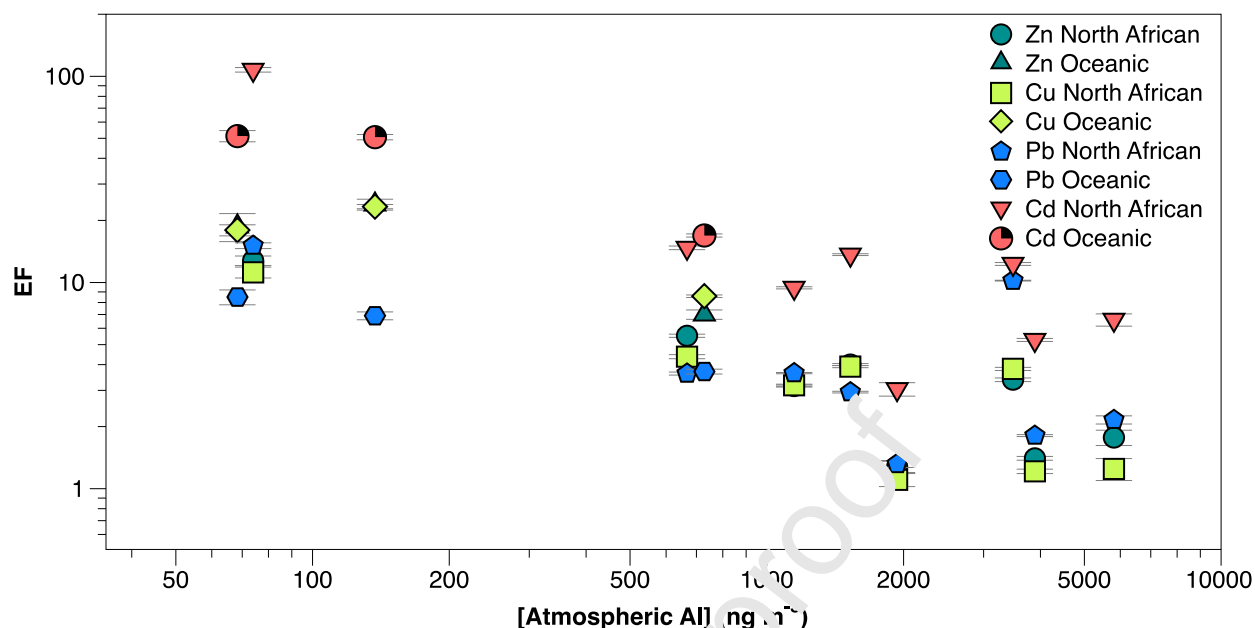
Figure 5: Log-log graph of the concentration of atmospheric Al plotted against enrichment factors of Zn, Cu, Cd and Pb in the same aerosol sample set (Cd: Bridgestock et al., 2017), (Pb: Bridgestock et al., 2016).
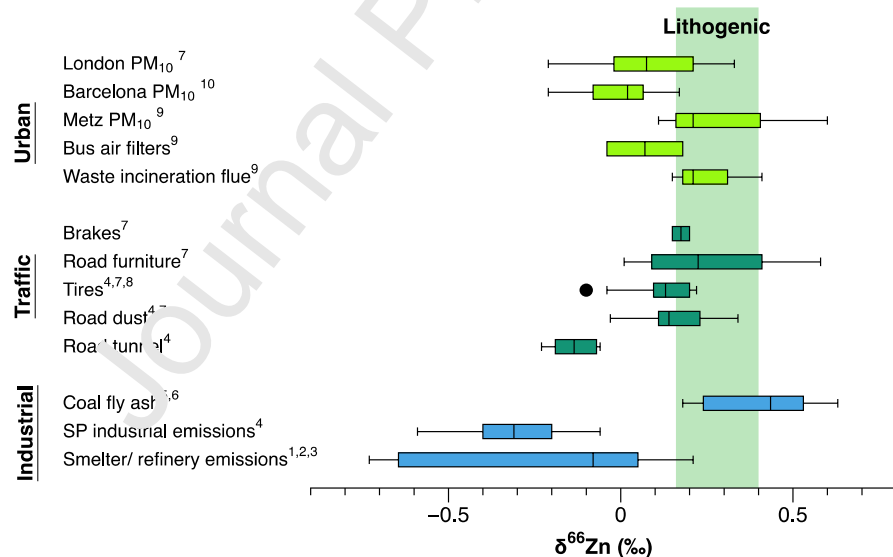
Figure 6: Plot of $\delta^{66}Zn_{JMC}$ values for anthropogenic reservoirs. SP refers to the city São Paulo. Green vertical shaded area gives range of lithogenic values for Zn +0.28 ± 0.12 ‰ from (Moynier et al., 2017). References: 1. (Mattielli et al., 2009), 2. (Bigalke et al., 2010), 3. (Gelly et al., 2019) 4. (Souto-Oliveira et al., 2018), 5. (Borrok et al., 2010), 6. (Novak et al., 2016), 7. (Dong et al., 2017), 8. (Thapalia et al., 2010), 9. (Cloquet et al., 2006a) 10. (Ochoa Gonzalez et al., 2016)
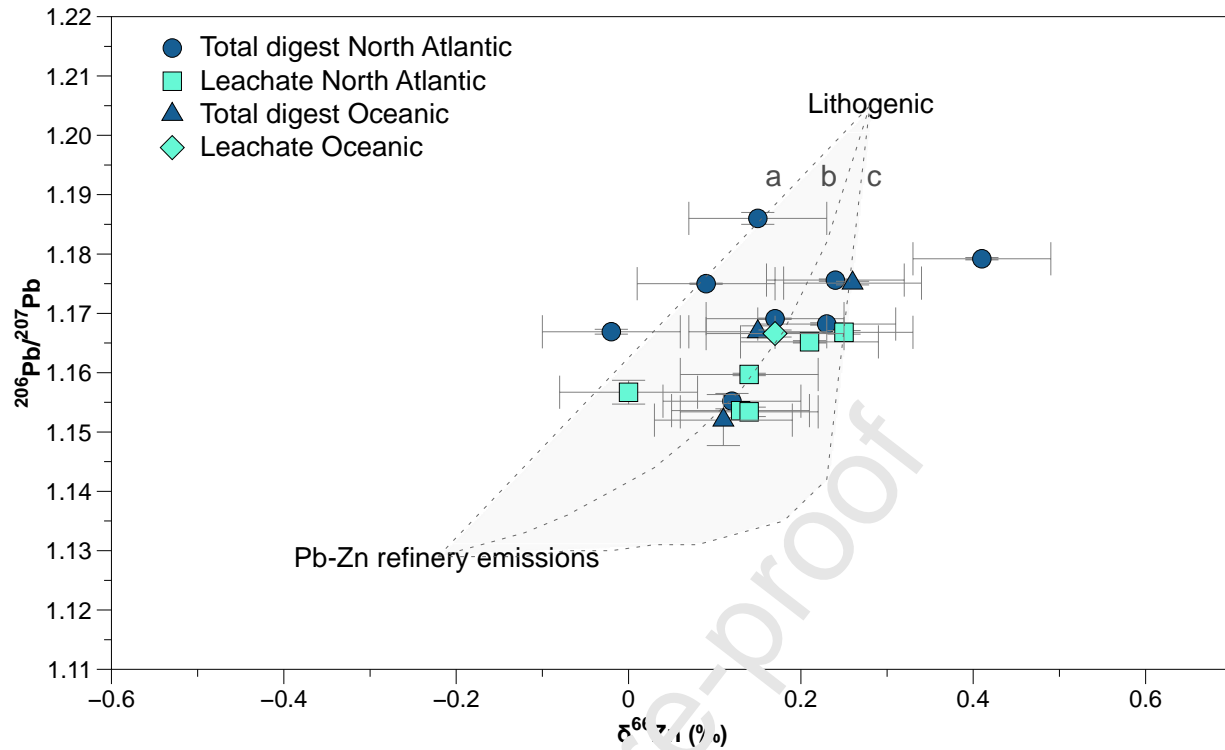
Figure 7: Aerosol Zn isotope compositions plotted against their ^{206}Pb/^{207}Pb isotope ratios (Bridgestock et al. 2016). Lithogenic values obtained from Moynier et al., (2017) for Zn (+0.28 ± 0.12‰) and Bridgestock, (2015; and references therein) for Pb (1.20504 ± 0.00458). Pb-Zn refinery emissions from Mattielli et al., (2009) for Zn (-0.22 ± 0.34‰) and (Cloquet et al., 2006b) for Pb (1.1289 ± 0.0022). The dashed lines labelled 'a', 'b' and 'c' are different, hypothetical, mixing lines. 'a' assumes equal parts Zn and Pb from the anthropogenic and lithogenic endmembers. 'b' and 'c' utilise a lithogenic Zn to Pb ratio of 3.94 (equivalent to UCC) and anthropogenic endmember Zn:Pb ratios of 1 for 'b' and 0.09 for 'c' (Cloquet et al., 2006b; Mattielli et al., 2009).

Declaration of interests

☐The authors declare that they have no known competing financial interests or personal relationships that could have appeared to influence the work reported in this paper.

☒The authors declare the following financial interests/personal relationships which may be considered as potential competing interests: